Communications in Analysis and Mechanics

https://www.aimspress.com/journal/cam

Communications in Analysis and Mechanics, 17(2): 630–661.
DOI: 10.3934/cam.2025025
Received: 17 February 2025
Revised: 22 May 2025
Accepted: 28 May 2025
Published: 18 June 2025

Research article

A second–order approximation scheme for Caputo–Hadamard derivative and its application in fractional Allen–Cahn equation

Luhan Sun, Zhen Wang*and Yabing Wei

School of Mathematical Sciences, Jiangsu University, Zhenjiang, 212013, P.R. China

* **Correspondence:** Email: wangzhen@ujs.edu.cn.

Abstract: In light of the advantages of the Caputo–Hadamard fractional derivative in characterizing ultra-slow diffusion phenomena, this paper proposes a second-order approximation scheme to approximate it. Then, for the Allen–Cahn equation with the Caputo–Hadamard fractional derivative in time, a numerical algorithm is designed. This algorithm employs the proposed second-order formula for time discretization. Considering the potential anisotropic behavior of the solution in space, the anisotropic nonconforming quasi-Wilson finite element method is utilized for spatial approximation. The error in the L^2-norm and the superclose error in the H^1-norm of this algorithm are analyzed. The global superconvergence in the H^1-norm is demonstrated through interpolation postprocessing techniques. Numerical examples are given to verify the theoretical results and further investigate the influence of different time derivatives on the dynamic behavior of the solution.

Keywords: Caputo–Hadamard derivative; L1$^+$ scheme; fractional Allen–Cahn equation; nonconforming FEM; superconvergence
Mathematics Subject Classification: 35R11, 65M12, 65M60

1. Introduction

Fractional calculus, an extension of classical calculus, offers a more precise and flexible tool for modeling complex phenomena by introducing fractional derivatives and integrals [1–3]. It demonstrates unique advantages in capturing memory effects and dealing with processes involving long-range dependencies, which are often difficult to accurately describe within the traditional framework of integer-order calculus. Hadamard's fractional calculus, proposed by Hadamard in 1892, shares similarities in form with the commonly used Riemann–Liouville integral/derivative and Caputo derivative, yet it has received relatively less attention. However, Hadamard's calculus can offer more accurate descriptions of phenomena such as Lomnitz's logarithmic creep law for specific substances [4] and ultra-slow diffusion processes [5]. For further applications of Hadamard's calculus, readers may refer to the literature [6–11].

It is widely acknowledged that determining exact solutions for fractional differential equations, irrespective of the type of fractional derivative involved, presents a significant challenge. Consequently, there has been an increased emphasis on researching numerical methods to address these solutions. In the context of Caputo–Hadamard fractional differential equations, scholars have devised several effective numerical approaches for their resolution. For instance, Li et al. employed the finite difference method as discussed in [12], while the local discontinuous Galerkin finite element method was explored in [13]. Zhao et al. introduced a spectral collocation method in [14]. Ou et al. examined the regularity and logarithmic decay of solutions to the Caputo–Hadamard fractional diffusion-wave equation in [15] and resolved it using the difference method. They later introduced a fitted scheme in [16], which demonstrated a convergence order of $\min\{2r\alpha, 2\}$, where r is the grading mesh parameter. Fan et al. proposed a series of approximation formulas for the Caputo–Hadamard fractional derivative in [5], including the L1-2 and L2-1$_\sigma$ formulas with the $(3-\alpha)$th order of convergence for $\alpha \in (0, 1)$, and the H2N2 formula also exhibiting the $(3-\alpha)$th order of convergence for $\alpha \in (1, 2)$. On the basis of the L1 and L2-1$_\sigma$ formulas approximating the Caputo derivative, Wang et al. [17, 18] extended them to the discrete Caputo–Hadamard derivative, also known as the L1 and L2-1$_\sigma$ formulas in the logarithmic sense. It is worth mentioning that the main difference between the Caputo–Hadamard derivative and the Caputo derivative lies in its integral kernel, which is composed of a logarithmic function. Therefore, if a logarithmic transformation is applied to the variable in the Caputo–Hadamard derivative, it can be converted into the corresponding Caputo analog [19–21]. Consequently, the approximation schemes in the aforementioned literature were derived under this idea. To provide approximation formulas specifically for the Caputo–Hadamard derivative, Wang et al. recently proposed the general L1 formula [22] and the L2-1$_\sigma$ formula [23], which, although similar in form to those in the logarithmic sense, differ in the selection of grid points. Mustapha [24] first introduced the time-stepping L1 scheme for discretizing the Riemann–Liouville fractional derivative, achieving second-order accuracy. Liao et al. proposed the L1$^+$ scheme for the Caputo derivative in [25], and subsequently established its discrete gradient structure in [26]. Since then, scholars have successfully applied this formula to the numerical solutions of many models and have gradually perfected its theoretical framework [27–29]. However, research on the Caputo–Hadamard fractional derivative has not yet been addressed. Therefore, the first task of this paper is to generalize it by constructing the L1$^+$ formula for the Caputo–Hadamard fractional derivative.

The Allen–Cahn equation is a significant nonlinear partial differential equation that plays a crucial role in explaining phase transition phenomena and addressing interfacial diffusion issues. This equation was initially proposed by Allen and Cahn [30], and it has been extensively studied in the field of nonlinear dynamics, demonstrating its broad application value in various domains such as materials science [31] and grain growth [32]. In an effort to better understand and describe the anomalous diffusion transport behavior in heterogeneous porous materials, scholars have introduced the time-fractional Allen–Cahn equation. Liu et al. [33] considered a finite difference approximation for the time-fractional Allen–Cahn equation. Liao et al. developed a series of efficient numerical schemes for solving the time-fractional Allen–Cahn equation, such as the backward Euler and stabilized semi-implicit scheme [34], the Crank-Nicolson-type scheme with variable steps [35], the variable-step L1 scheme preserving a compatible energy law [36], and the nonuniform L2-1$_\sigma$ scheme [37]. Huang and Stynes [38] employed the Alikhanov L2-1$_\sigma$ scheme and a standard finite element method (FEM) to solve the time-fractional Allen–Cahn equation. Fan and Li numerically solved the Allen–Cahn equation with different time

derivatives [39]. In this paper, we consider the following time-fractional Allen–Cahn equation:

$$\begin{cases} {}_{CH}\mathrm{D}^{\alpha}_{a,t}u(\mathbf{x},t) - \Delta u(\mathbf{x},t) + \dfrac{1}{\epsilon^2}f(u(\mathbf{x},t)) = 0, & (\mathbf{x},t) \in \Omega \times (a,T], \\ u(\mathbf{x},t) = 0, & (\mathbf{x},t) \in \partial\Omega \times [a,T], \\ u(\mathbf{x},a) = u_a(\mathbf{x}), & \mathbf{x} \in \Omega, \end{cases} \tag{1.1}$$

where $\Omega \subset \mathbb{R}^2$ represents a bounded rectangular domain with the boundary $\partial\Omega$. The nonlinear term $f(u) = u^3 - u$ with $u_a(\mathbf{x})$ is the initial function, and ${}_{CH}\mathrm{D}^{\alpha}_{a,t}$ is the Caputo–Hadamard fractional derivative of order α, which is defined as [40]

$${}_{CH}\mathrm{D}^{\alpha}_{a,t}v(t) = \int_a^t \omega_{1-\alpha}(\log t - \log s)\delta v(s)\frac{\mathrm{d}s}{s},\ 0 < \alpha < 1,\ 0 < a < t,$$

with $\omega_\beta(t) = \frac{t^{\beta-1}}{\Gamma(\beta)}$ and $\delta^n v(s) = \left(s\frac{\mathrm{d}}{\mathrm{d}s}\right)^n v(s) = \delta(\delta^{n-1}v(s))$, and $\forall n \in \mathbb{Z}^+$.

The nonconforming FEM boasts several advantages, including the ability to handle complex geometries and the flexibility of adaptive mesh refinement. It is well-known that the nonconforming Wilson element exhibits superior convergence properties compared with the conforming bilinear element. However, the Wilson element only converges on rectangular and parallelogram meshes. To enhance its applicability, modifications to the Wilson element have been attempted, as seen in [41], among others. Specifically, Jiang and Cheng introduced a quasi-Wilson element in [42], whose shape functions are independent of the element's geometric shape and converge on arbitrary quadrilateral meshes. Therefore, the second task of this paper is to apply the nonconforming quasi-Wilson FEM to the numerical solution of the time-fractional Allen–Cahn equation (1.1). It is widely recognized that solutions to time-fractional partial differential equations may exhibit a weak singularity at the initial time [43, 44]. Additionally, it is crucial to note that the solution may display anisotropic behavior in space, meaning that the solution changes significantly only in certain directions while varying slowly in others. In such cases, using anisotropic meshes can reduce computational effort and clearly reflect the anisotropic characteristics of the solution. Consequently, we will employ an anisotropic nonconforming quasi-Wilson FEM for the spatial discretization of Eq. (1.1), and for the temporal direction, we will use the $\mathrm{L1}^+$ formula approximation. We will analyze the error in the L^2-norm, the superclose property in the H^1-norm, and the global superconvergence in the H^1-norm. Finally, we provide numerical examples to validate the theoretical results and simulate solutions to the Allen–Cahn equation with different time derivatives, observing the impact of the time derivative on the solution's behavior.

The structure of this paper is as follows. In Section 2, we propose a nonuniform $\mathrm{L1}^+$ formula for approximating the Caputo–Hadamard derivative and conduct a detailed analysis of its truncation error. Through a specific constructive example, we verify the convergence and numerical accuracy of this formula. In Section 3, we combine the spatially nonconforming finite element method with the $\mathrm{L1}^+$ formula on a nonuniform time mesh to obtain the fully–discrete scheme of Eq. (1.1). We analyze the L^2-norm error and the H^1-norm superclose estimate of this scheme, and further give the global superconvergence estimate in the H^1-norm. In Section 4, we provide some numerical examples to test the correctness of the theoretical analysis in Section 3. The last section is the conclusion.

2. Nonuniform L1$^+$ approximation for Caputo–Hadamard fractional derivative

Throughout the paper, C denotes a generic constant that can take different values in different places but is independent of the mesh parameters. The notation $A \approx B$ means that a constant C exists such that $A = CB$. For a given finite time T, let $\mathcal{I}_t = \{I_n = (t_{n-1}, t_n)\}_{n=1}^N$ be a partition of (a, T), where $a = t_0 < t_1 < \cdots < t_N = T$, $t_n = a + (T-a)(n/N)^r$, and the grading mesh parameter $r \geq 1$. From [22], we know that

$$\tau_n = t_n - t_{n-1} = (T-a)N^{-r}(n^r - (n-1)^r) \leq C(T-a)N^{-r}n^{r-1},\ 1 \leq n \leq N, \tag{2.1}$$

$$\begin{aligned} C\left(\frac{T-a}{T}\right)N^{-r}n^{r-1} &\leq \log t_n - \log t_{n-1} \\ &= \log\left(1 + \frac{\tau_n}{t_{n-1}}\right) \leq C\left(\frac{T-a}{a}\right)N^{-r}n^{r-1},\ 2 \leq n \leq N, \end{aligned} \tag{2.2}$$

$$\begin{aligned} C\frac{(T-a)n^rN^{-r}}{T} &\leq \log t_n - \log a \\ &= \log\left(1 + \frac{(T-a)n^rN^{-r}}{a}\right) \leq C\frac{(T-a)n^rN^{-r}}{a},\ 1 \leq n \leq N. \end{aligned} \tag{2.3}$$

2.1. Nonuniform L1$^+$ discretization

Let $\Pi_{\log}v(t)$ represent the linear interpolation function of $v(t)$ in the interval $[t', t'']$, i.e.,

$$\Pi_{\log}v(t) = \frac{\log t'' - \log t}{\log t'' - \log t'}v(t') + \frac{\log t - \log t'}{\log t'' - \log t'}v(t''). \tag{2.4}$$

Writing $v^n = v(t_n)$, we then present the L1$^+$ discretization for the Caputo–Hadamard fractional derivative at time $t = t_n$,

$$\begin{aligned} &\frac{1}{\log t_n - \log t_{n-1}}\int_{t_{n-1}}^{t_n} {}_{CH}\mathrm{D}_{a,t}^{\alpha}v\frac{\mathrm{d}t}{t} \\ &\quad\approx \frac{1}{\log t_n - \log t_{n-1}}\int_{t_{n-1}}^{t_n}\int_a^t \omega_{1-\alpha}(\log t - \log s)\delta(\Pi_{\log}v(s))\frac{\mathrm{d}s}{s}\frac{\mathrm{d}t}{t} \\ &\quad= \frac{1}{\log t_n - \log t_{n-1}}\int_{t_{n-1}}^{t_n}\sum_{k=1}^{n}\int_{t_{k-1}}^{\min\{t_k,t\}} \omega_{1-\alpha}(\log t - \log s)\frac{v^k - v^{k-1}}{\log t_k - \log t_{k-1}}\frac{\mathrm{d}s}{s}\frac{\mathrm{d}t}{t} \\ &\quad= \sum_{k=1}^{n} b_{n-k}^n(v^k - v^{k-1}), \end{aligned} \tag{2.5}$$

where

$$b_0^n = \frac{1}{(\log t_n - \log t_{n-1})^2}\int_{t_{n-1}}^{t_n}\int_{t_{n-1}}^{t} \omega_{1-\alpha}(\log t - \log s)\frac{\mathrm{d}s}{s}\frac{\mathrm{d}t}{t} = \frac{1}{\Gamma(3-\alpha)(\log t_n - \log t_{n-1})^{\alpha}},$$

$$b_{n-k}^n = \frac{1}{(\log t_n - \log t_{n-1})}\frac{1}{(\log t_k - \log t_{k-1})}\int_{t_{n-1}}^{t_n}\int_{t_{k-1}}^{t_k} \omega_{1-\alpha}(\log t - \log s)\frac{\mathrm{d}s}{s}\frac{\mathrm{d}t}{t}$$

$$= \frac{1}{(\log t_n - \log t_{n-1})}\frac{1}{(\log t_k - \log t_{k-1})}\Big[\omega_{3-\alpha}(\log t_n - \log t_{k-1}) - \omega_{3-\alpha}(\log t_n - \log t_k)$$
$$+ \omega_{3-\alpha}(\log t_{n-1} - \log t_k) - \omega_{3-\alpha}(\log t_{n-1} - \log t_{k-1})\Big],\ 1 \le k \le n-1.$$

For simplicity, we write

$$_{CH}\delta^{\alpha}_{a,t} v^n = \sum_{k=1}^{n} b^n_{n-k}(v^k - v^{k-1}). \tag{2.6}$$

Set $\rho_n = \frac{\log t_{n-1} - \log t_{n-2}}{\log t_n - \log t_{n-1}}$ for $n = 2, 3, \cdots, N$. Our grid partition implies that $0 < \rho_n \le 1$.

Lemma 1. *Regarding b^n_{n-k}, $1 \le k \le n \le N$. We have the following properties:*
(i) Assume $\alpha \ge (5 - \sqrt{17})/2 \approx 0.43845$, if $\rho_n \ge \frac{2(1-\alpha)}{\alpha(3-\alpha)}$ for $1 \le n \le N$, we have

$$b^n_0 > b^n_1 > \cdots > b^n_{n-1} > 0.$$

(ii) $b^n_{n-k} \ge \frac{1}{(2-\alpha)(\log t_k - \log t_{k-1})}\int_{t_{k-1}}^{t_k} \omega_{1-\alpha}(\log t_n - \log s)\frac{\mathrm{d}s}{s}$, $1 \le k \le n \le N$.

Proof. Part (i) can be obtained along the same lines as in Section 5 of [29].

Next, we prove that Part (ii) holds. According to the definition of b^n_{n-k} $(1 \le k \le n)$, when $k = n$, the result can be obtained directly. When $1 \le k \le n-1$, a $\xi_n \in (t_{n-1}, t_n)$ exists such that

$$\begin{aligned} b^n_{n-k} &= \frac{1}{(\log t_n - \log t_{n-1})(\log t_k - \log t_{k-1})}\int_{t_{n-1}}^{t_n}\int_{t_{k-1}}^{t_k} \omega_{1-\alpha}(\log t - \log s)\frac{\mathrm{d}s}{s}\frac{\mathrm{d}t}{t} \\ &= \frac{1}{(\log t_n - \log t_{n-1})(\log t_k - \log t_{k-1})}\int_{t_{k-1}}^{t_k}\int_{t_{n-1}}^{t_n} \omega_{1-\alpha}(\log t - \log s)\frac{\mathrm{d}t}{t}\frac{\mathrm{d}s}{s} \\ &= \frac{1}{\log t_k - \log t_{k-1}}\int_{t_{k-1}}^{t_k} \omega_{1-\alpha}(\log \xi_n - \log s)\frac{\mathrm{d}s}{s} \\ &\ge \frac{1}{(2-\alpha)(\log t_k - \log t_{k-1})}\int_{t_{k-1}}^{t_k} \omega_{1-\alpha}(\log t_n - \log s)\frac{\mathrm{d}s}{s}. \end{aligned}$$

The proof has been completed. □

2.2. Truncation error analysis of L1$^+$ scheme

In this subsection, we analyze the truncation error of the L1$^+$ formula. For $t \in (a, T]$, suppose $u(t)$ satisfies the initial weak singularity condition

$$|\delta^l v(t)| \le C\left(1 + (\log t - \log a)^{\sigma - l}\right),\ \text{ for } l = 0, 1, 2, 3,\ \sigma \in (0, 1). \tag{2.7}$$

Assume that

$$R^n_1 = \frac{1}{\log t_n - \log t_{n-1}}\int_{t_{n-1}}^{t_n}\int_a^t \omega_{1-\alpha}(\log t - \log s)\delta(v - \Pi_{\log} v)(s)\frac{\mathrm{d}s}{s}\frac{\mathrm{d}t}{t},\ 1 \le n \le N. \tag{2.8}$$

For $1 \le n \le N$ and $t \in I_n$, let $\psi(t) = v(t) - \Pi_{\log} v(t)$. We can then obtain the following from (2.8)

$$\begin{aligned} R^n_1 &= \frac{1}{\log t_n - \log t_{n-1}}\int_{t_{n-1}}^{t_n}\int_a^t \omega_{1-\alpha}(\log t - \log s)\delta\psi(s)\frac{\mathrm{d}s}{s}\frac{\mathrm{d}t}{t} \\ &= \frac{1}{\log t_n - \log t_{n-1}}\Big[\int_a^{t_n} \omega_{1-\alpha}(\log t_n - \log s)\psi(s)\frac{\mathrm{d}s}{s} \\ &\qquad - \int_a^{t_{n-1}} \omega_{1-\alpha}(\log t_{n-1} - \log s)\psi(s)\frac{\mathrm{d}s}{s}\Big]. \end{aligned} \tag{2.9}$$

For $2 \le n \le N$ and $t \in I_n$, according to the mean value theorem, $\xi_n \in I_n$ exists such that

$$\psi(t) = \frac{1}{2}\delta^2 v(\xi_n) \log \frac{t}{t_{n-1}} \log \frac{t}{t_n}. \tag{2.10}$$

For $n = 1$, since $v(t)$ satisfies the condition (2.7), $\delta v(t)$ may blow up as $t \to a^+$. Therefore, it needs to be estimated separately. Utilizing (2.4), we have

$$\begin{aligned} |\psi(t)| &= \left| v(t) - \frac{\log t_1 - \log t}{\log t_1 - \log a} v(a) - \frac{\log t - \log a}{\log t_1 - \log a} v(t_1) \right| \\ &= \left| \frac{\log t_1 - \log t}{\log t_1 - \log a} (v(t) - v(a)) - \frac{\log t - \log a}{\log t_1 - \log a} (v(t_1) - v(t)) \right| \\ &= \left| \frac{\log t_1 - \log t}{\log t_1 - \log a} \int_a^t \delta v(s) \frac{\mathrm{d}s}{s} - \frac{\log t - \log a}{\log t_1 - \log a} \int_t^{t_1} \delta v(s) \frac{\mathrm{d}s}{s} \right| \\ &\le \int_a^{t_1} |\delta v(s)| \frac{\mathrm{d}s}{s} \le C(\log t_1 - \log a)^{\sigma}, \ \forall t \in (a, t_1), \end{aligned} \tag{2.11}$$

which further yields

$$\left| \frac{1}{\log t_1 - \log a} \int_a^{t_1} \psi(s) \frac{\mathrm{d}s}{s} \right| \le \max_{a \le t \le t_1} |\psi(t)| \le C(\log t_1 - \log a)^{\sigma}. \tag{2.12}$$

For $1 \le n \le N$, let

$$\Phi = \Phi(n, N, r, \alpha, \sigma) = \begin{cases} N^{-2}(\log t_n - \log a)^{\sigma - \alpha - 2/r}, & r(\sigma + 1) > 2, \\ N^{-r(1+\sigma)}(\log t_n - \log a)^{-1-\alpha} \log (n+1), & r(\sigma + 1) = 2, \\ N^{-r(1+\sigma)}(\log t_n - \log a)^{-1-\alpha}, & r(\sigma + 1) < 2. \end{cases} \tag{2.13}$$

Our next task is to prove that

$$|R_1^n| \le C\Phi, \quad 1 \le n \le N. \tag{2.14}$$

From (2.3), it follows that for $r(1 + \sigma) \le 2$, we have

$$\begin{aligned} N^{-2}(\log t_n - \log a)^{\sigma - \alpha - 2/r} &= N^{-2}(\log t_n - \log a)^{-1-\alpha}(\log t_n - \log a)^{1+\sigma-2/r} \\ &\approx N^{-2}(\log t_n - \log a)^{-1-\alpha}(n/N)^{r(1+\sigma-2/r)} \\ &\le N^{-r(1+\sigma)}(\log t_n - \log a)^{-1-\alpha}. \end{aligned}$$

Therefore, to prove that (2.14) is true, it suffices to show that

$$|R_1^n| \le CN^{-2}(\log t_n - \log a)^{\sigma - \alpha - 2/r} \ \text{ for } \ r \ge 1. \tag{2.15}$$

Next, we will prove that (2.15) holds for different values of n through several lemmas.

Lemma 2. *For $r \ge 1$, when $n = 1, 2, 3$, we have $|R_1^n| \le C\Phi$.*

Proof. When $n = 1$, by applying inequality (2.12), we can deduce that

$$\begin{aligned}|R_1^1| &= \frac{1}{\log t_1 - \log a}\int_a^{t_1} \omega_{1-\alpha}(\log t_1 - \log s)\psi(s)\frac{\mathrm{d}s}{s}\\ &\le \max_{a\le t\le t_1}|\psi(t)|\frac{1}{\log t_1 - \log a}\int_a^{t_1} \omega_{1-\alpha}(\log t_1 - \log s)\frac{\mathrm{d}s}{s}\\ &\le C(\log t_1 - \log a)^{\sigma-\alpha} \le CN^{-2}(\log t_1 - \log a)^{\sigma-\alpha-2/r}.\end{aligned}$$

For the case of $n = 2$, using $\log t_2 - \log t_1 \approx \log t_1 - \log a$ along with the inequality (2.11), we can similarly infer that

$$\begin{aligned}|R_1^2| &= \frac{1}{\log t_2 - \log t_1}\left|\int_a^{t_1}\Big(\omega_{1-\alpha}(\log t_2 - \log s) - \omega_{1-\alpha}(\log t_1 - \log s)\Big)\psi(s)\frac{\mathrm{d}s}{s}\right.\\ &\quad\left.+\int_{t_1}^{t_2}\omega_{1-\alpha}(\log t_2 - \log s)\psi(s)\frac{\mathrm{d}s}{s}\right|\\ &\le C\frac{(\log t_1 - \log a)^{\sigma}}{\log t_2 - \log t_1}\int_a^{t_1}\Big(\omega_{1-\alpha}(\log t_1 - \log s) - \omega_{1-\alpha}(\log t_2 - \log s)\Big)\frac{\mathrm{d}s}{s}\\ &\quad + C(\log t_2 - \log t_1)(\log t_1 - \log a)^{\sigma-2}\int_{t_1}^{t_2}\omega_{1-\alpha}(\log t_2 - \log s)\frac{\mathrm{d}s}{s}\\ &\le C(\log t_2 - \log t_1)^{\sigma-\alpha} \le CN^{-2}(\log t_2 - \log t_1)^{\sigma-\alpha-2/r}.\end{aligned}$$

When $n = 3$, the proof process is analogous to the case of $n = 2$, ultimately yielding

$$\begin{aligned}|R_1^3| &= \frac{1}{\log t_3 - \log t_2}\left|\int_a^{t_1}[\omega_{1-\alpha}(\log t_3 - \log s) - \omega_{1-\alpha}(\log t_2 - \log s)]\psi(s)\frac{\mathrm{d}s}{s}\right.\\ &\quad\left.+\int_{t_1}^{t_2}[\omega_{1-\alpha}(\log t_3 - \log s) - \omega_{1-\alpha}(\log t_2 - \log s)]\psi(s)\frac{\mathrm{d}s}{s} + \int_{t_2}^{t_3}\omega_{1-\alpha}(\log t_3 - \log s)\psi(s)\frac{\mathrm{d}s}{s}\right|\\ &\le C\frac{(\log t_1 - \log a)^{\sigma}}{\log t_3 - \log t_2}\int_a^{t_1}[\omega_{1-\alpha}(\log t_3 - \log s) - \omega_{1-\alpha}(\log t_2 - \log s)]\frac{\mathrm{d}s}{s}\\ &\quad + \frac{(\log t_1 - \log a)^{\sigma-2}(\log t_2 - \log t_1)^2}{\log t_3 - \log t_2}\int_{t_1}^{t_2}\left(\omega_{1-\alpha}(\log t_3 - \log s) - \omega_{1-\alpha}(\log t_2 - \log s)\right)\frac{\mathrm{d}s}{s}\\ &\quad + \frac{(\log t_2 - \log a)^{\sigma-2}(\log t_3 - \log t_2)^2}{\log t_3 - \log t_2}\int_{t_2}^{t_3}\omega_{1-\alpha}(\log t_3 - \log s)\frac{\mathrm{d}s}{s}\\ &\le C(\log t_3 - \log a)^{\sigma-\alpha} \le CN^{-2}(\log t_3 - \log a)^{\sigma-\alpha-2/r},\end{aligned}$$

where $\xi_1 \in (a, t_1)$ and $\xi_2 \in (t_1, t_2)$. By combining the estimated results of these three scenarios and employing (2.15), the proof of this lemma can be completed. □

Lemma 3. *For $r \ge 1$, when $n \ge 4$, $|R_1^n| \le C\Phi$ is true.*

Proof. Firstly, we decompose R_1^n into $R_1^n := R_{11}^n + R_{12}^n + R_{13}^n$, where

$$R_{11}^n = \frac{1}{\log t_n - \log t_{n-1}}\sum_{k=1}^{n_0}\int_{t_{k-1}}^{t_k}\left(\omega_{1-\alpha}(\log t_n - \log s) - \omega_{1-\alpha}(\log t_{n-1} - \log s)\right)\psi(s)\frac{\mathrm{d}s}{s}, \tag{2.16}$$

$$R_{12}^n = \frac{1}{\log t_n - \log t_{n-1}} \int_{t_{n_0}}^{t_{n_0+1}} \omega_{1-\alpha}(\log t_n - \log s)\psi(s)\frac{\mathrm{d}s}{s}, \tag{2.17}$$

$$R_{13}^n = \frac{1}{\log t_n - \log t_{n-1}} \left[\int_{t_{n_0+1}}^{t_n} \omega_{1-\alpha}(\log t_n - \log s)\psi(s)\frac{\mathrm{d}s}{s} - \int_{t_{n_0}}^{t_{n-1}} \omega_{1-\alpha}(\log t_{n-1} - \log s)\psi(s)\frac{\mathrm{d}s}{s} \right], \tag{2.18}$$

with $n_0 = [n/2]$. We then prove one by one that for $i = 1, 2, 3$, $|R_{1i}^n| \le C\Phi$ holds.

Step 1: From (2.16), we can deduce that a $\xi_n \in (t_{n-1}, t_n)$ exists such that

$$\begin{aligned}
|R_{11}^n| &\le C \sum_{k=1}^{n_0} \int_{t_{k-1}}^{t_k} \omega_{-\alpha}(\log \xi_n - \log s)|\psi(s)|\frac{\mathrm{d}s}{s} \\
&\le C(\log t_1 - \log a)^{\sigma} \int_a^{t_1} \omega_{-\alpha}(\log \xi_n - \log s)\frac{\mathrm{d}s}{s} \\
&\quad + C \sum_{k=2}^{n_0} (\log t_k - \log t_{k-1})^2 (\log t_{k-1} - \log a)^{\sigma-2} \int_{t_{k-1}}^{t_k} \omega_{-\alpha}(\log \xi_2 - \log s)\frac{\mathrm{d}s}{s} \\
&\le C(\log t_1 - \log a)^{\sigma+1} (\log t_{n-1} - \log t_1)^{-\alpha-1} \\
&\quad + C \sum_{k=2}^{n_0} (\log t_k - \log t_{k-1})^3 (\log t_{k-1} - \log a)^{\sigma-2} (\log t_{n-1} - \log t_{n_0})^{-\alpha-1} \\
&\le C(\log t_1 - \log a)^{\sigma+1} (\log t_n - \log a)^{-\alpha-1} \\
&\quad + C \sum_{k=2}^{n_0} (\log t_k - \log t_{k-1})^3 (\log t_{k-1} - \log a)^{\sigma-2} (\log t_n - \log a)^{-\alpha-1},
\end{aligned}$$

where for the last inequality, we have utilized $\log t_{n-1} - \log a \approx \log t_n - \log a$, $(\log t_n - \log t_1)^{-\alpha-1} = (\log t_n - \log a - (\log t_1 - \log a))^{-\alpha-1} \le C(\log t_n - \log a)^{-\alpha-1}$, and $\log t_{n-1} - \log t_{n_0} = C(N^{-r}((n-1)^r - [n/2]^r)) \ge C(\log t_n - \log a)$.

Since

$$\begin{aligned}
(\log t_k - \log t_{k-1})^3 (\log t_{k-1} - \log a)^{\sigma-2} &\le C(k-1)^{r(\sigma-2)} N^{-r(\sigma-2)} (\log t_k - \log t_{k-1})^3 \\
&\le Ck^{(r-1)(\sigma-2)} N^{-r(\sigma-2)} k^{\sigma-2} (\log t_k - \log t_{k-1})^3 \\
&\le Ck^{\sigma-2} (\log t_k - \log t_{k-1})^{\sigma+1},
\end{aligned}$$

we can obtain

$$\begin{aligned}
|R_{11}^n| &\le C(\log t_1 - \log a)^{\sigma+1} (\log t_n - \log a)^{-\alpha-1} \\
&\quad + C(\log t_n - \log a)^{-\alpha-1} \sum_{k=2}^{n_0} k^{\sigma-2} (\log t_k - \log t_{k-1})^{\sigma+1} \\
&\le C(\log t_n - \log a)^{-\alpha-1} N^{-r(1+\sigma)} \sum_{k=1}^{n_0} k^{r(1+\sigma)-3}
\end{aligned}$$

$$\leq C(\log t_n - \log a)^{-\alpha-1} N^{-r(1+\sigma)} \times \begin{cases} n^{r(1+\sigma)-2}, & r(1+\sigma) > 2, \\ \log n, & r(1+\sigma) = 2, \\ 1, & r(1+\sigma) < 2. \end{cases}$$

Furthermore, according to $(\log t_n - \log a)^{1+\sigma} \approx (n/N)^{r(1+\sigma)}$ and $(\log t_n - \log a)^{-2/r} \approx n^{-2}N^2$, we can see that $|R_{11}^n| \leq C\Phi$.

Step 2: Using (2.1)–(2.3), one can derive $\log t_{n_0} - \log a \approx (\log t_n - \log a)$ for $n \geq 1$, and $\log t_n - \log t_{n_0+1} \geq C(\log t_n - \log a)$ for $n \geq 4$. From (2.10), we obtain

$$\begin{aligned} |R_{12}^n| &= \left| \frac{1}{\log t_n - \log t_{n-1}} \int_{t_{n_0}}^{t_{n_0+1}} \omega_{1-\alpha}(\log t_n - \log s)\psi(s)\frac{\mathrm{d}s}{s} \right| \\ &\leq C\frac{1}{\log t_n - \log t_{n-1}}(\log t_n - \log t_{n_0+1})^{-\alpha}(\log t_{n_0+1} - \log t_{n_0})^3(\log t_{n_0} - \log a)^{\sigma-2} \\ &\leq C\frac{1}{\log t_n - \log t_{n-1}}(\log t_n - \log a)^{-\alpha}(\log t_n - \log t_{n-1})^3(\log t_n - \log a)^{\sigma-2} \\ &= (\log t_n - \log t_{n-1})^2(\log t_n - \log a)^{\sigma-\alpha-2} \\ &\approx N^{-2}(\log t_n - \log a)^{\sigma-\alpha-2/r}, \end{aligned} \tag{2.19}$$

which, combined with (2.15), implies that $|R_{12}^n| \leq C\Phi$.

Step 3: Let

$$\begin{aligned} r^k = &\frac{1}{\log t_n - \log t_{n-1}}\Big(\int_{t_k}^{t_{k+1}} \omega_{1-\alpha}(\log t_n - \log s)\psi(s)\frac{\mathrm{d}s}{s} \\ &- \int_{t_{k-1}}^{t_k} \omega_{1-\alpha}(\log t_{n-1} - \log s)\psi(s)\frac{\mathrm{d}s}{s}\Big), \end{aligned} \tag{2.20}$$

and

$$\begin{aligned} \overline{r}^k = &\frac{\delta^2 u(t_k)}{2(\log t_n - \log t_{n-1})}\Big(\int_{t_k}^{t_{k+1}} (\log s - \log t_k)(\log s - \log t_{k+1})\omega_{1-\alpha}(\log t_n - \log s)\frac{\mathrm{d}s}{s} \\ &- \int_{t_{k-1}}^{t_k} (\log s - \log t_{k-1})(\log s - \log t_k)\omega_{1-\alpha}(\log t_{n-1} - \log s)\frac{\mathrm{d}s}{s}\Big). \end{aligned} \tag{2.21}$$

From (2.18), we can derive $R_{13}^n = \sum_{k=n_0+1}^{n-1} r^k$. Applying the weak singularity condition (2.7), it follows that for $j = k,\ k+1$, a $\xi_j \in (t_{j-1}, t_j)$ exists such that

$$\begin{aligned} |\delta^2 v(\xi_j) - \delta^2 v(t_k)| &\leq (\log t_j - \log t_{j-1}) \max_{t_{j-1} \leq s \leq t_{j+1}} |\delta^3 v(s)| \\ &\leq C(\log t_n - \log t_{n-1})(\log t_n - \log a)^{\sigma-3}. \end{aligned} \tag{2.22}$$

Combining (2.20)–(2.22), we deduce that

$$\begin{aligned} |r^k - \overline{r}^k| \leq\ & C(\log t_n - \log a)^{\sigma-3}(\log t_n - \log t_{n-1})^2 \\ &\times \left(\int_{t_k}^{t_{k+1}} \omega_{1-\alpha}(\log t_n - \log s)\frac{\mathrm{d}s}{s} + \int_{t_{k-1}}^{t_k} \omega_{1-\alpha}(\log t_{n-1} - \log s)\frac{\mathrm{d}s}{s} \right), \end{aligned}$$

which further yields

$$\begin{aligned}
&\sum_{k=n_0+1}^{n-1} |r^k - \overline{r}^k| \\
&\leq C(\log t_n - \log a)^{\sigma-3}(\log t_n - \log t_{n-1})^2 \\
&\quad \times \left(\int_{t_{n_0+1}}^{t_n} \omega_{1-\alpha}(\log t_n - \log s)\frac{\mathrm{d}s}{s} + \int_{t_{n_0}}^{t_{n-1}} \omega_{1-\alpha}(\log t_{n-1} - \log s)\frac{\mathrm{d}s}{s} \right) \\
&\leq C(\log t_n - \log t_{n-1})^2(\log t_n - \log a)^{\sigma-\alpha-2} \leq C\Phi.
\end{aligned} \tag{2.23}$$

Next, we aim to estimate $\sum_{k=n_0+1}^{n-1} \overline{r}^k$. To achieve this, we initially divide it into

$$\sum_{k=n_0+1}^{n-1} \overline{r}^k := \sum_{k=n_0+1}^{n-1} \overline{r}_1^k + \sum_{k=n_0+1}^{n-1} \overline{r}_2^k, \tag{2.24}$$

where

$$\begin{aligned}
\overline{r}_1^k =& \frac{\delta^2 v(t_k)}{2(\log t_n - \log t_{n-1})} \Big(\int_{\frac{t_{k+1}t_{k-1}}{t_k}}^{t_{k+1}} (\log s - \log t_k)(\log s - \log t_{k+1})\omega_{1-\alpha}(\log t_n - \log s)\frac{\mathrm{d}s}{s} \\
&- \int_{t_{k-1}}^{t_k} (\log s - \log t_{k-1})(\log s - \log t_k)\omega_{1-\alpha}(\log t_{n-1} - \log s)\frac{\mathrm{d}s}{s} \Big),
\end{aligned} \tag{2.25}$$

$$\overline{r}_2^k = \frac{\delta^2 v(t_k)}{2(\log t_n - \log t_{n-1})} \int_{t_k}^{\frac{t_{k+1}t_{k-1}}{t_k}} (\log s - \log t_k)(\log s - \log t_{k+1})\omega_{1-\alpha}(\log t_n - \log s)\frac{\mathrm{d}s}{s}. \tag{2.26}$$

To estimate $\sum_{k=n_0+1}^{n-1} \overline{r}_1^k$, we first perform a substitution for s with $s = s + \log t_{k+1} - \log t_k$ in (2.25). Then, $\overline{r}_1^k$ can be rewritten as

$$\begin{aligned}
\overline{r}_1^k =& \frac{\delta^2 v(t_k)}{2(\log t_n - \log t_{n-1})} \\
&\times \int_{t_{k-1}}^{t_k} (\log s + \log t_{k+1} - \log t_k - \log t_k)(\log s - \log t_k) \\
&\times \omega_{1-\alpha}(\log t_n - \log s - (\log t_{k+1} - \log t_k))\frac{\mathrm{d}s}{s} \\
&- \frac{\delta^2 v(t_k)}{2(\log t_n - \log t_{n-1})} \int_{t_{k-1}}^{t_k} (\log s - \log t_{k-1})(\log s - \log t_k)\omega_{1-\alpha}(\log t_{n-1} - \log s)\frac{\mathrm{d}s}{s} \\
:=& \overline{r}_{11}^k + \overline{r}_{12}^k,
\end{aligned} \tag{2.27}$$

where

$$\begin{aligned}
\overline{r}_{11}^k =& \frac{\delta^2 v(t_k)}{2(\log t_n - \log t_{n-1})} \int_{t_{k-1}}^{t_k} (\log s - \log t_{k-1})(\log s - \log t_k) \\
&\times \left(\omega_{1-\alpha}\left(\log t_n - \log s - (\log t_{k+1} - \log t_k)\right) - \omega_{1-\alpha}(\log t_{n-1} - \log s) \right) \frac{\mathrm{d}s}{s},
\end{aligned}$$

$$\widetilde{r}_{12}^{k} = \frac{\delta^2 v(t_k)}{2(\log t_n - \log t_{n-1})} \int_{t_{k-1}}^{t_k} (\log t_{k+1} - \log t_k - \log t_k + \log t_{k-1})(\log s - \log t_k) \times \omega_{1-\alpha}\left(\log t_n - \log s - (\log t_{k+1} - \log t_k)\right) \frac{\mathrm{d}s}{s}.$$

Since $\widetilde{r}_{11}^{n-1} = 0$, we only need to estimate $\widetilde{r}_{11}^{k}$ for $n_0 + 1 \le k \le n-2$. From (2.7), we have

$$\begin{aligned}
|\widetilde{r}_{11}^{k}| &\le C(\log t_n - \log t_{n-1})(\log t_n - \log a)^{\sigma-2} \\
&\quad \times \int_{t_{k-1}}^{t_k} \left(\omega_{1-\alpha}(\log t_{n-1} - \log s) - \omega_{1-\alpha}\left(\log t_n - \log s - (\log t_{k+1} - \log t_k)\right)\right) \frac{\mathrm{d}s}{s} \\
&\le C(\log t_n - \log t_{n-1})^2 (\log t_n - \log a)^{\sigma-2} N^{-r} n^{r-2} \\
&\quad \times (n-k)\left((n-k-1)(n-1)^{r-1}\right)^{-\alpha-1} N^{r(\alpha+1)} \\
&\approx C(\log t_n - \log t_{n-1})^2 (\log t_n - \log a)^{\sigma-2} N^{r\alpha} n^{-r\alpha+\alpha-1} (n-k)^{-\alpha}.
\end{aligned}$$

Then we can bound the first term as follows:

$$\begin{aligned}
\sum_{k=n_0+1}^{n-1} |\widetilde{r}_{11}^{k}| &\le C(\log t_n - \log t_{n-1})^2 (\log t_n - \log a)^{\sigma-2} N^{r\alpha} n^{-r\alpha+\alpha-1} \sum_{k=n_0+1}^{n-2} (n-k)^{-\alpha} \\
&\le C(\log t_n - \log t_{n-1})^2 (\log t_n - \log a)^{\sigma-2} N^{r\alpha} n^{-r\alpha} \\
&\le C(\log t_n - \log t_{n-1})^2 (\log t_n - \log a)^{\sigma-\alpha-2} \\
&\le CN^{-2} (\log t_n - \log a)^{\sigma-\alpha-2/r}.
\end{aligned} \tag{2.28}$$

For the second term $\widetilde{r}_{12}^{k}$, we can show that

$$\begin{aligned}
\left| \sum_{k=n_0+1}^{n-1} \widetilde{r}_{12}^{k} \right| &\le C \sum_{k=n_0+1}^{n-1} N^{-r}((k+1)^{r-1} - (k-1)^{r-1})(\log t_n - \log a)^{\sigma-2} \\
&\quad \times \int_{t_{k-1}}^{t_k} \omega_{1-\alpha}\left(\log t_n - \log s - (\log t_{k+1} - \log t_k)\right) \frac{\mathrm{d}s}{s} \\
&\le CN^{-r} n^{r-2} (\log t_n - \log a)^{\sigma-2} \\
&\quad \times \int_{t_{n_0}}^{t_{n-1}} \omega_{1-\alpha}\left(\log t_n - \log s - (\log t_{k+1} - \log t_k)\right) \frac{\mathrm{d}s}{s} \\
&\le CN^{-r} n^{r-2} (\log t_n - \log a)^{\sigma-2} \omega_{2-\alpha}(\log t_n - \log t_{n_0}) \\
&\le CN^{-2} (\log t_n - \log a)^{\sigma-\alpha-2/r}.
\end{aligned} \tag{2.29}$$

Substituting (2.28) and (2.29) into (2.27), we know from (2.15) that

$$\left| \sum_{k=n_0+1}^{n-1} \widetilde{r}_{1}^{k} \right| \le C\Phi. \tag{2.30}$$

Finally, the estimation of $\sum_{k=n_0+1}^{n-1} \widetilde{r}_{2}^{k}$ remains unaddressed. Applying (2.19) and noticing that $\log t_{k+1} -$

$\log t_k - (\log t_k - \log t_{k-1}) \le CN^{-r}n^{r-2} \le CN^{-2}(\log t_n - \log a)^{1-2/r}$ yields

$$\begin{aligned}\left|\sum_{k=n_0+1}^{n-1} \widetilde{r}_2^k\right| &\le C \sum_{k=n_0+1}^{n-1} \frac{(\log t_k - \log a)^{\sigma-2}}{2(\log t_n - \log t_{n-1})} (\log t_{k+1} - \log t_k - (\log t_k - \log t_{k-1})) \\ &\quad \times (\log t_k - \log t_{k-1}) \int_{t_k}^{\frac{t_{k+1}t_{k-1}}{t_k}} \omega_{1-\alpha}(\log t_n - \log s)\frac{\mathrm{d}s}{s} \\ &\le CN^{-2}(\log t_n - \log a)^{\sigma-1-2/r} \int_{t_{n_0+1}}^{t_n} \omega_{1-\alpha}(\log t_n - \log s)\frac{\mathrm{d}s}{s} \\ &\le CN^{-2}(\log t_n - \log a)^{\sigma-\alpha-2/r} \le C\Phi.\end{aligned} \tag{2.31}$$

Combining (2.24), (2.30), and (2.31), we can obtain

$$\sum_{k=n_0+1}^{n-1} \widetilde{r}^k \le C\Phi,$$

which, together with (2.23) and the triangle inequality, leads to

$$|R_{13}^n| \le \sum_{k=n_0+1}^{n-1} |r^k| \le C\Phi.$$

By synthesizing the conclusions of Steps 1–3, we have completed the proof of the lemma. □

Theorem 1. *When $r \ge 1$, for $n = 1, 2, \cdots, N$, it holds that*

$$|R_1^n| \le C\Phi. \tag{2.32}$$

Proof. The conclusion of the theorem can be directly derived from Lemmas 2 and 3. □

Next, we present an example to validate the error and convergence order of the proposed nonuniform L1$^+$ formula (2.5).

Example 1. *We solve the following fractional differential equation numerically:*

$$\begin{cases} {}_{CH}\mathrm{D}_{1,t}^{\alpha} y(t) = f(t), \ t \in (1, 2], \ \alpha \in (0, 1), \\ y(1) = 0, \end{cases}$$

where the exact solution is $y(t) = (\log t)^{\alpha} + (\log t)^3$, and the function $f(t)$ can be directly computed.

It is clear that when $\sigma = \alpha$, $y(t)$ satisfies the initial weak singularity condition (2.7). Let Y^n be an approximation of $y(t)$ at $t = t_n$, in which case, we have the following approximation scheme:

$$\begin{cases} {}_{CH}\delta_{a,t}^{\alpha} Y^n = \frac{f(t_n)+f(t_{n-1})}{2}, \ 1 \le n \le N, \\ Y^0 = y(1). \end{cases}$$

Analogous to the analysis process in Theorem 6.2 of [29], it can be shown that the maximum norm error

$$\max_{1\le n\le N} |y(t_n) - Y^n| \le CN^{-\min\{r\alpha,2\}}.$$

Figure 1 illustrates the maximum norm errors and numerical accuracy for various values of α when the grading mesh parameter $r = 1$. Clearly, the numerical accuracy is $O(N^{-\alpha})$. When $r = \frac{2}{\alpha}$, the numerical results are shown in Figure 2, in which second-order convergence can be observed. These results align with the conclusions of Theorem 1.

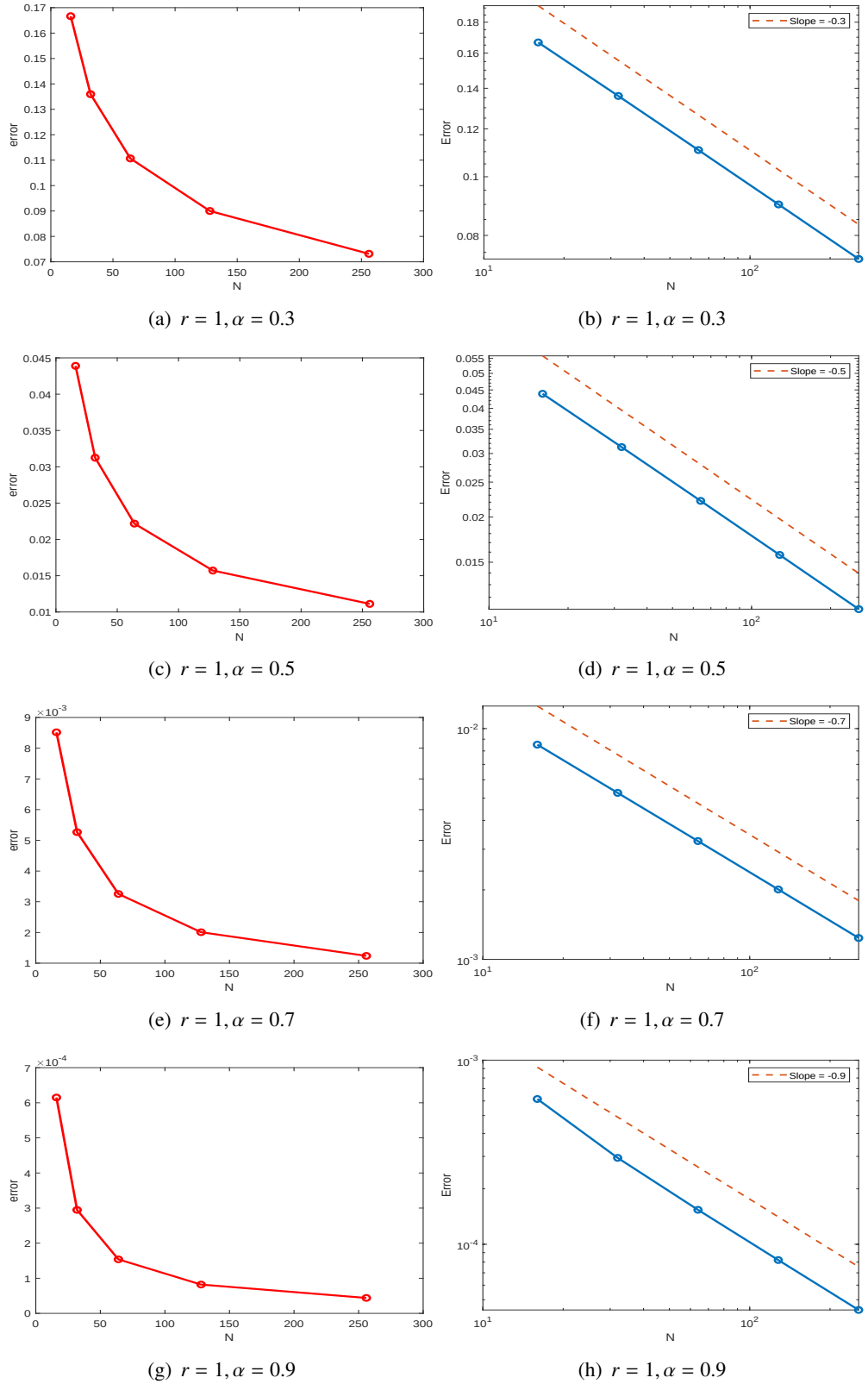

(a) $r = 1, \alpha = 0.3$ (b) $r = 1, \alpha = 0.3$

(c) $r = 1, \alpha = 0.5$ (d) $r = 1, \alpha = 0.5$

(e) $r = 1, \alpha = 0.7$ (f) $r = 1, \alpha = 0.7$

(g) $r = 1, \alpha = 0.9$ (h) $r = 1, \alpha = 0.9$

Figure 1. The maximum norm errors and convergence orders under different values of α (Example 1).

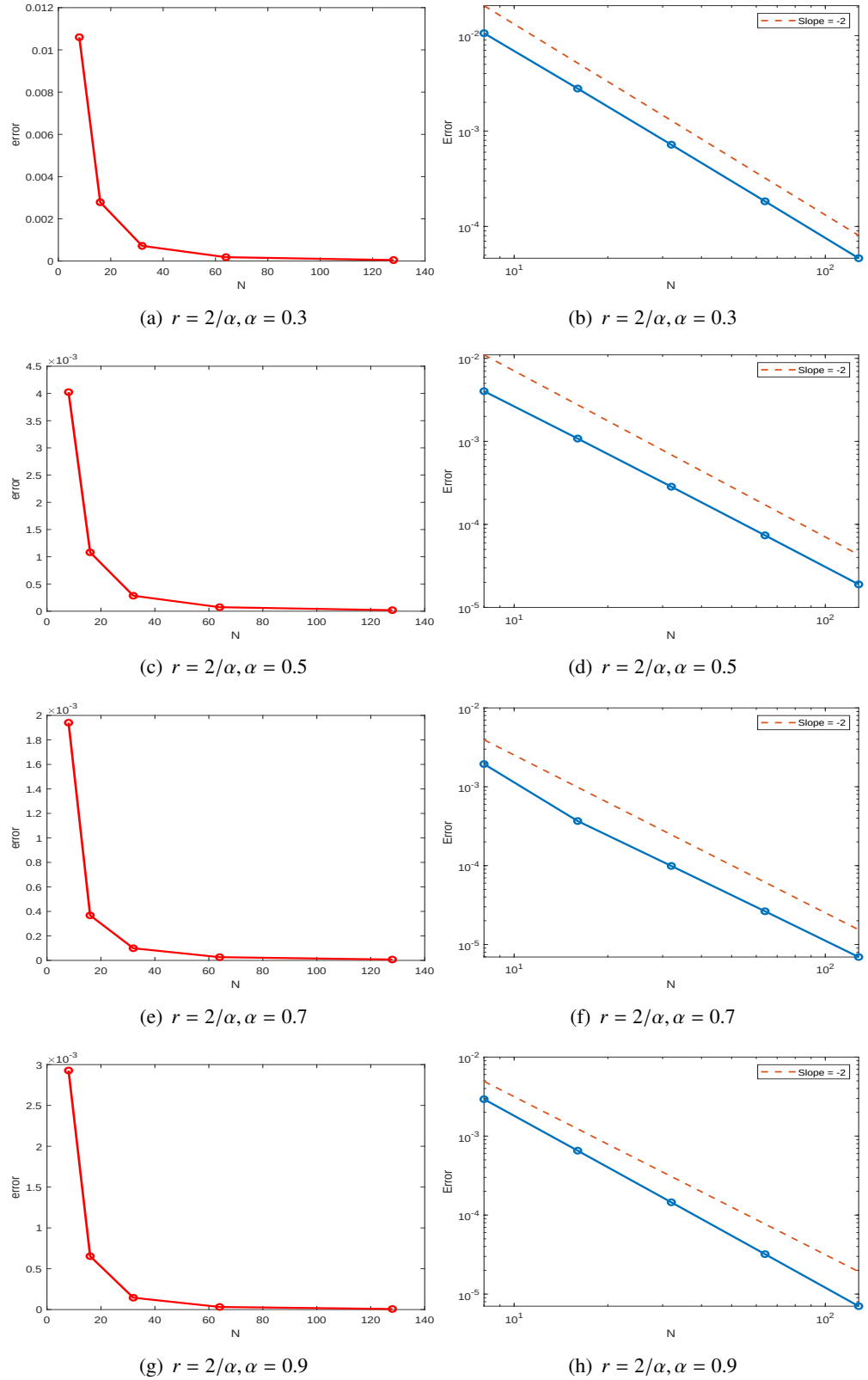

(a) $r = 2/\alpha, \alpha = 0.3$ (b) $r = 2/\alpha, \alpha = 0.3$

(c) $r = 2/\alpha, \alpha = 0.5$ (d) $r = 2/\alpha, \alpha = 0.5$

(e) $r = 2/\alpha, \alpha = 0.7$ (f) $r = 2/\alpha, \alpha = 0.7$

(g) $r = 2/\alpha, \alpha = 0.9$ (h) $r = 2/\alpha, \alpha = 0.9$

Figure 2. The maximum norm errors and convergence orders under different values of α (Example 1).

3. The fully–discrete numerical scheme for the problem (1.1)

In the spatial domain, let $(\cdot,\cdot)$ denote the L^2-inner product on Ω, and let $\|\cdot\|$ represent the corresponding L^2-norm. For a non-negative integer p, we define $H^p(\Omega)$ as the Sobolev space with the norm $\|\cdot\|_p$ and the seminorm $|\cdot|_p$.

3.1. Anisotropic nonconforming quasi-Wilson FEM

We utilize Γ_h to stand for a rectangular partition of the domain Ω, with $\overline{\Omega}$ being the union of all elements e in Γ_h, i.e., $\overline{\Omega} = \cup_{e\in\Gamma_h} e$. For any element $e \in \Gamma_h$, let $O_e = (x_e, y_e)$ represent its center. The lengths of the two edges of e in the x and y directions are denoted $2h_{x,e}$ and $2h_{y,e}$, respectively. Here, Γ_h is a family of anisotropic grids without any regularity or quasi-uniform assumptions. In other words, Γ_h is not required to satisfy $\frac{h_{x,e}}{h_{y,e}} \le C$ or $\frac{h_e}{h_{y,e}} \le C$, where $h_e = \max\{h_{x,e}, h_{y,e}\}$, and $h = \max_{e\in\Gamma_h}\{h_e\}$.

Assume that $\hat{e} = [-1,-1]^2$ is the reference element on the $\hat{x} - \hat{y}$ plane. Its four vertices are $\hat{a}_1 = (-1,-1)$, $\hat{a}_2 = (1,-1)$, $\hat{a}_3 = (1,1)$, and $\hat{a}_4 = (-1,1)$. Similar to the work in [45, 46], we define the nonconforming quasi-Wilson finite element $\{\hat{e}, \hat{P}, \hat{\Sigma}\}$ as follows:

$$\hat{P} = \text{span}\Big\{N_i(\hat{x},\hat{y}), i = 1,2,3,4,\ \hat{\Psi}(\hat{x}),\ \hat{\Psi}(\hat{y})\Big\},\ \hat{\Sigma} = \{\hat{v}_1, \hat{v}_2, \hat{v}_3, \hat{v}_4, \hat{v}_5, \hat{v}_6\},$$

where $N_i(\hat{x},\hat{y}) = \frac{1}{4}(1+\hat{x}_i\hat{x})(1+\hat{y}_i\hat{y})$, with $(\hat{x}_1,\hat{x}_2,\hat{x}_3,\hat{x}_4) = (-1,1,1,-1)$ and $(\hat{y}_1,\hat{y}_2,\hat{y}_3,\hat{y}_4) = (-1,-1,1,1)$; $\hat{\Psi}(s) = \frac{1}{2}(s^2-1) - \frac{5}{12}(s^4-1)$. Also, $\hat{v}_i = \hat{v}(\hat{A}_i)\,(i = 1,2,3,4)$, $\hat{v}_5 = \frac{1}{|\hat{e}|}\int_{\hat{e}} \frac{\partial^2\hat{v}}{\partial\hat{x}^2}\mathrm{d}\hat{x}\mathrm{d}\hat{y}$, and $\hat{v}_6 = \frac{1}{|\hat{e}|}\int_{\hat{e}} \frac{\partial^2\hat{v}}{\partial\hat{y}^2}\mathrm{d}\hat{x}\mathrm{d}\hat{y}$. For any $\hat{v} \in \hat{P}$, the associated interpolation can be uniquely expressed as $\hat{I}_h\hat{v}(\hat{x},\hat{y}) = \sum_{i=1}^4 N_i(\hat{x},\hat{y})\hat{v}_i + \hat{\Psi}(\hat{x})\hat{v}_5 + \hat{\Psi}(\hat{y})\hat{v}_6$. The affine mapping $F_e : \hat{e} \to e$ is defined by $x = x_e + h_{x,e}\hat{x}$ and $y = y_e + h_{y,e}\hat{y}$.

We define the finite element space by

$$V_h = \Big\{v_h : v_h|_e = \hat{v}\circ F_e^{-1},\ \hat{v}\in\hat{P},\ v_h(s) = 0,\ \text{for every node point } s \text{ on } \partial\Omega\Big\}.$$

For any given $v_h = \bar{v}_h + \tilde{v}_h$, with $\bar{v}_h$ and $\tilde{v}_h$ denoting the conforming and nonconforming components of V_h respectively. As can be obtained from [47], we have

$$\|\nabla v_h\|^2 = \|\nabla\bar{v}_h\|^2 + \|\nabla\tilde{v}_h\|^2,\ \|\tilde{v}_h\| \le Ch\|\nabla\tilde{v}_h\|.$$

The Ritz projection, denoted $R_h : H_0^1(\Omega) \to V_h$, is defined in such a way that for any $v_h \in V_h$, the equation

$$(\nabla(v - R_h v), \nabla v_h) = 0$$

holds. Let $I_h : H^1(\Omega) \to V_h$ be an interpolation operator satisfying $I_h|_e = I_e$ and $I_e v = \hat{I}_h\hat{v}\circ F_e^{-1}$. The L^2-projection operator $P_h : L^2(\Omega) \to V_h$ and the discrete Laplacian operator $\Delta_h : V_h \to V_h$ are defined as

$$(P_h v, v_h) = (v, v_h),\ \forall v_h \in V_h, \quad (\Delta_h w_h, v_h) = -(\nabla w_h, \nabla v_h),\ \forall w_h, v_h \in V_h, \tag{3.1}$$

respectively. According to [48], it is known that

$$(\Delta_h R_h v, v_h) = (P_h\Delta v, v_h) - \sum_e \int_{\partial e} \frac{\partial v}{\partial\vec{n}} v_h \mathrm{d}s,\ \forall v \in H^2(\Omega),\ v_h \in V_h, \tag{3.2}$$

where $\vec{n}$ is the unit outward normal vector on ∂e.

Lemma 4 ([49]). *For $v \in H_0^1(\Omega) \cap H^2(\Omega)$, it is true that*

$$\|R_h v - v\| + h\|\nabla(R_h v - v)\| \le Ch^2\|v\|_2. \tag{3.3}$$

If $v \in H_0^1(\Omega) \cap H^3(\Omega)$, one can derive

$$\|R_h v - I_h v\|_1 \le C\|v\|_3. \tag{3.4}$$

If $v \in H_0^1(\Omega) \cap H^4(\Omega)$, one has

$$(\nabla(v - R_h v), \nabla v_h) \le Ch^2\|v\|_4\|v_h\|, \quad \left|\sum_e \int_{\partial e} \frac{\partial v}{\partial \vec{n}} v_h \mathrm{d}s\right| \le Ch^2\|v\|_4\|v_h\|, \ \forall v_h \in V_h. \tag{3.5}$$

Integrating the first equation of (1.1) over the time interval I_n, we obtain

$$\int_{t_{n-1}}^{t_n} {}_{CH}\mathrm{D}_{a,t}^{\alpha} u(\mathbf{x}, t)\frac{\mathrm{d}t}{t} - \int_{t_{n-1}}^{t_n} \Delta u(\mathbf{x}, t)\frac{\mathrm{d}t}{t} + \frac{1}{\epsilon^2}\int_{t_n-1}^{t_n} (u^3(\mathbf{x}, t) - u(\mathbf{x}, t))\frac{\mathrm{d}t}{t} = 0.$$

For simplicity, let $\overline{g^n} = \frac{1}{\log t_n - \log t_{n-1}} \int_{t_{n-1}}^{t_n} g(t)\frac{\mathrm{d}t}{t}$. Then the equation above can be rewritten as

$$\overline{{}_{CH}\mathrm{D}_{a,t}^{\alpha} u^n} - \overline{\Delta u^n} + \frac{1}{\epsilon^2}\overline{(u^n)^3} - \frac{1}{\epsilon^2}\overline{u^n} = 0, \tag{3.6}$$

where $u^n = u(\mathbf{x}, t_n)$ for $0 \le n \le N$. For the nonlinear term $(u^n)^3$, we employ the Newton linearization method (see, e.g., [38]), namely $(u^n)^3 \approx (u^{n-1})^3 + 3(u^{n-1})^2(u^n - u^{n-1})$, to derive the time semi-discrete scheme

$$\begin{cases} {}_{CH}\delta_{a,t}^{\alpha} u^n - \Delta u^{n-\frac{1}{2}} - \frac{1}{\epsilon^2} u^{n-\frac{1}{2}} + \frac{1}{\epsilon^2} H(u^n) = 0, \\ u^0 = u_a, \end{cases}$$

where $H(u^n) = (u^{n-1})^3 + \frac{3}{2}(u^{n-1})^2(u^n - u^{n-1})$, and $u^{n-\frac{1}{2}} = (u^n + u^{n-1})/2$.

On the basis of (3.1) and the equation above, we can now describe the fully–discrete numerical scheme to find $\{U_h^n\}_{n=0}^N \in V_h$ such that

$$\begin{cases} \left({}_{CH}\delta_{a,t}^{\alpha} U_h^n, v_h\right) + \left(\nabla U_h^{n-1/2}, \nabla v_h\right) - \frac{1}{\epsilon^2}(U_h^{n-\frac{1}{2}}, v_h) + \frac{1}{\epsilon^2}\left(H(U_h^n), v_h\right) = 0, \ \forall v_h \in V_h, \\ U_h^0(\mathbf{x}) = R_h u_a(\mathbf{x}), \ \forall \mathbf{x} \in \Omega, \end{cases} \tag{3.7}$$

where $U_h^n = U_h(t_n)$ and $U_h^{n-1/2} = \frac{U_h^n + U_h^{n-1}}{2}$.

3.2. Global superconvergence analysis

In this subsection, we discuss the convergence of the scheme (3.7) under the L^2-norm and the superclose convergence under the H^1-norm. Subsequently, on the basis of the interpolation postprocessing technique defined in [50], we analyze the global superconvergence of this scheme under the H^1-norm. Suppose that the solution u in (1.1) satisfies the following regularity condition:

$$\begin{aligned} &u(\mathbf{x}, t) \in L^{\infty}(a, T; H_0^1(\Omega) \cap H^4(\Omega)), \quad u(\mathbf{x}, \cdot) \in C[a, T] \cap C^3(a, T], \\ &\left\|\delta^l u(\mathbf{x}, \cdot)\right\|_2 \le C(1 + (\log t - \log a)^{\sigma - l}), \quad l = 0, 1, 2, 3, \quad \sigma \in (0, 1). \end{aligned} \tag{3.8}$$

Lemma 5. *Assume*

$$R_2^n = \overline{\Delta u^n} - \Delta u^{n-\frac{1}{2}} + \frac{1}{\epsilon^2}\left(\overline{u^n} - u^{n-\frac{1}{2}}\right),\ R_3^n = \frac{1}{\epsilon^2}\left(\overline{(u^n)^3} - (u^{n-1})^3 + \frac{3}{2}(u^{n-1})^2(u^n - u^{n-1})\right).$$

Under the condition (3.8)*, a constant C exists such that*

$$\begin{aligned}
&\|\nabla R_2^n\| \le C(\log t_n - \log a)^{-\sigma} N^{-\min\{2,r\sigma\}}, \quad 1 \le n \le N;\\
&\|\nabla R_3^n\| \le C(\log t_n - \log a)^{-\sigma} N^{-\min\{2,r\sigma\}}, \quad 1 \le n \le N.
\end{aligned}$$

Proof. From [29], it follows that $H(u^n)$ provides a second-order approximation for the nonlinear term $\frac{1}{\log t_n - \log t_{n-1}} \int_{t_{n-1}}^{t_n} \left(u(t) - u^3(t)\right) \frac{\mathrm{d}t}{t}$.

On the basis of (2.10)–(2.12), we readily derive

$$\begin{aligned}
&\left|\frac{1}{\log t_n - \log t_{n-1}} \int_{t_{n-1}}^{t_n} u(t)\frac{\mathrm{d}t}{t} - \frac{u^n + u^{n-1}}{2}\right|\\
&= \frac{\int_{t_{n-1}}^{t_n} \left(u(t) - \Pi_{\log} u(t)\right) \frac{\mathrm{d}t}{t}}{\log t_n - \log t_{n-1}}\\
&= \left|\frac{1}{\log t_n - \log t_{n-1}} \int_{t_{n-1}}^{t_n} \psi(t)\frac{\mathrm{d}t}{t}\right|\\
&\le (\log t_n - \log t_{n-1})^2 (\log t_n - \log a)^{\sigma - 2/r}.
\end{aligned}$$

Combining this result with Lemmas 3.1 and 3.2 in [23], we obtain the desired conclusion. □

Theorem 2. *Suppose u and* $\{U_h^n\}_{n=1}^N$ *are the solutions of equations* (1.1) *and* (3.7)*, respectively. Assume that u satisfies the conditions in* (3.8) *and* ${}_{CH}\mathrm{D}_{a,t}^{\alpha} u \in L^{\infty}(a, T; H^2(\Omega))$*. Then the following estimates hold*

$$\|u^n - U_h^n\| \le C(h^2 + N^{-\min\{2,r\sigma\}}),\ \|\nabla(I_h u^n - U_h^n)\| \le C(h^2 + N^{-\min\{2,r\sigma\}}).$$

Proof. To begin, let $u^n - U_h^n = R_h u^n - U_h^n + u^n - R_h u^n := \xi^n + \eta^n$. By applying (3.5)-(3.7), we derive that

$$\begin{aligned}
&({}_{CH}\delta_{a,t}^{\alpha}\xi^n, v_h) - (\Delta_h \xi^{n-\frac{1}{2}}, v_h)\\
=&(R_{hCH}\delta_{a,t}^{\alpha}u^n, v_h) - ({}_{CH}\delta_{a,t}^{\alpha}U_h^n, v_h) - (\Delta_h R_h u^{n-\frac{1}{2}}, v_h) + (\Delta_h U_h^{n-\frac{1}{2}}, v_h)\\
=&((R_h - P_h)_{CH}\delta_{a,t}^{\alpha}u^n, v_h) + \left(P_h(\frac{1}{\epsilon^2}\overline{u^n} - \frac{1}{\epsilon^2}\overline{(u^n)^3} - R_1^n), v_h\right) + \left(P_h(\overline{\Delta u^n} - \Delta u^{n-\frac{1}{2}}), v_h\right)\\
&- \frac{1}{\epsilon^2}(P_h U_h^{n-\frac{1}{2}}, v_h) + \frac{1}{\epsilon^2}\left(P_h((U_h^{n-1})^3 + \frac{3}{2}(U_h^{n-1})^2(U_h^n - U_h^{n-1})), v_h\right)\\
&+ \sum_e \int_{\partial e} \frac{\partial u^{n-\frac{1}{2}}}{\partial \vec{n}} v_h \mathrm{d}s\\
=&-(P_{hCH}\delta_{a,t}^{\alpha}\eta^n, v_h) - (P_h R_1^n, v_h) + \frac{1}{\epsilon^2}(P_h(\overline{u^n} - u^{n-\frac{1}{2}}), v_h)\\
&+ \left(P_h(\overline{\Delta u^n} - \Delta u^{n-\frac{1}{2}}), v_h\right) + \frac{1}{\epsilon^2}(P_h(u^{n-\frac{1}{2}} - U_h^{n-\frac{1}{2}}), v_h)\\
&- \frac{1}{\epsilon^2}\left(P_h(\overline{(u^n)^3} - (u^{n-1})^3 - \frac{3}{2}(u^{n-1})^2(u^n - u^{n-1})), v_h\right)\\
&- \frac{1}{\epsilon^2}\left(P_h((u^{n-1})^3 + \frac{3}{2}(u^{n-1})^2(u^n - u^{n-1})), v_h\right)\\
&+ \frac{1}{\epsilon^2}\left(P_h((U_h^{n-1})^3 + \frac{3}{2}(U_h^{n-1})^2(U_h^n - U_h^{n-1})), v_h\right) + \sum_e \int_{\partial e} \frac{\partial u^{n-\frac{1}{2}}}{\partial \vec{n}} v_h \mathrm{d}s.
\end{aligned} \tag{3.9}$$

Notice that

$$\begin{aligned}
&(u^{n-1})^3 + \frac{3}{2}(u^{n-1})^2(u^n - u^{n-1}) - (U_h^{n-1})^3 - \frac{3}{2}(U_h^{n-1})^2(U_h^n - U_h^{n-1})\\
=&(u^{n-1})^3 - (U_h^{n-1})^3 + \frac{3}{2}((u^{n-1})^2 - (U_h^{n-1})^2)(u^n - u^{n-1}) + \frac{3}{2}(U_h^{n-1})^2(u^n - U_h^n - u^{n-1} + U_h^{n-1})\\
=&((u^{n-1})^2 + (U_h^{n-1})^2 + u^{n-1}U_h^{n-1} + \frac{3}{2}(u^{n-1} + U_h^{n-1})(u^n - u^{n-1}) - \frac{3}{2}(U_h^{n-1})^2)(u^{n-1} - U_h^{n-1})\\
&+ \frac{3}{2}(U_h^{n-1})^2(u^n - U_h^n).
\end{aligned}$$

From (3.9), we then get

$$\begin{aligned}
&({}_{CH}\delta_{a,t}^{\alpha}\xi^n, v_h) - (\Delta_h \xi^{n-\frac{1}{2}}, v_h)\\
&\quad= \left(P_h(-{}_{CH}\delta_{a,t}^{\alpha}\eta^n - R_1^n + R_2^n - R_3^n - \frac{1}{\epsilon^2}\Phi^n + \frac{1}{\epsilon^2}u^{n-\frac{1}{2}} - \frac{1}{\epsilon^2}U_h^{n-\frac{1}{2}}), v_h\right)\\
&\qquad+ \sum_e \int_{\partial e} \frac{\partial u^{n-\frac{1}{2}}}{\partial \vec{n}} v_h \mathrm{d}s,
\end{aligned} \tag{3.10}$$

where $\Phi^n = \Phi_1^n(\xi^{n-1} + \eta^{n-1}) + \Phi_2^n(\xi^n + \eta^n)$, $\Phi_1^n = ((u^{n-1})^2 + (U_h^{n-1})^2 + u^{n-1}U_h^{n-1} + \frac{3}{2}(u^n - u^{n-1})(u^{n-1} + U_h^{n-1}) - \frac{3}{2}(U_h^{n-1})^2$, and $\Phi_2^n = \frac{3}{2}(U_h^{n-1})^2$.

Taking $v_h = 2\xi^{n-\frac{1}{2}}$ in (3.10), we obtain

$$\begin{aligned}
&2({}_{CH}\delta^{\alpha}_{a,t}\xi^n, \xi^{n-\frac{1}{2}}) + 2\|\nabla\xi^{n-\frac{1}{2}}\|^2 \\
&\quad = \Big(P_h\big(-{}_{CH}\delta^{\alpha}_{a,t}\eta^n - R_1^n + R_2^n - R_3^n + \frac{1}{\epsilon^2}(\frac{1}{2} - \Phi_1^n)(\xi^{n-1} + \eta^{n-1}) \\
&\qquad + \frac{1}{\epsilon^2}(\frac{1}{2} - \Phi_2^n)(\xi^n + \eta^n)\big), 2\xi^{n-\frac{1}{2}}\Big) + 2\sum_e \int_{\partial e} \frac{\partial u^{n-\frac{1}{2}}}{\partial \vec{n}} \xi^{n-\frac{1}{2}} \mathrm{d}s.
\end{aligned} \tag{3.11}$$

Applying Lemma A.1 in Appendix, one can get

$$2({}_{CH}\delta^{\alpha}_{a,t}\xi^n, \xi^{n-\frac{1}{2}}) \geq \sum_{k=1}^{n} b_{n-k}^n(\|\xi^k\|^2 - \|\xi^{k-1}\|^2), \ 1 \leq n \leq N. \tag{3.12}$$

Substituting (3.12) into (3.11) and noting that

$$\begin{aligned}
-{}_{CH}\delta^{\alpha}_{a,t}\eta^n - R_1^n &= -(\overline{{}_{CH}\mathrm{D}^{\alpha}_{a,t}u^n} - R_1^n - R_h\overline{{}_{CH}\mathrm{D}^{\alpha}_{a,t}u^n} + R_hR_1^n) - R_1^n \\
&= -\overline{{}_{CH}\mathrm{D}^{\alpha}_{a,t}\eta^n} - R_hR_1^n,
\end{aligned}$$

we have

$$\begin{aligned}
&\sum_{k=1}^{n} b_{n-k}^n(\|\xi^k\|^2 - \|\xi^{k-1}\|^2) + 2\|\nabla\xi^{n-\frac{1}{2}}\|^2 \\
&\quad \leq \Big(P_h\big(-\overline{{}_{CH}\mathrm{D}^{\alpha}_{a,t}\eta^n} + \frac{1}{\epsilon^2}(\frac{1}{2} - \Phi_1^n)(\xi^{n-1} + \eta^{n-1}) + \frac{1}{\epsilon^2}(\frac{1}{2} - \Phi_2^n)(\xi^n + \eta^n)\big), 2\xi^{n-\frac{1}{2}}\Big) \\
&\qquad + \Big(P_h\big(-R_hR_1^n + R_2^n - R_3^n, 2\xi^{n-\frac{1}{2}}\big)\Big) + 2\sum_e \int_{\partial e} \frac{\partial u^{n-\frac{1}{2}}}{\partial \vec{n}} \xi^{n-\frac{1}{2}} \mathrm{d}s.
\end{aligned} \tag{3.13}$$

Utilizing the Sobolev embedding theorem, we find that a constant C exists such that $\|u^n\|_{L^\infty(\Omega)} \leq C$. Following a similar argument to that in [51, Theorem 3.2], it can be shown that U_h^n for $1 \leq n \leq N$ satisfies $\|U_h^n\| \leq C$. Using (3.2) together with the definition of η^n and an application of the Cauchy–Schwarz inequality yields

$$\begin{aligned}
&\Big|\Big(P_h\big(-\overline{{}_{CH}\mathrm{D}^{\alpha}_{a,t}\eta^n} + \frac{1}{\epsilon^2}(\frac{1}{2} - \Phi_1^n)(\xi^{n-1} + \eta^{n-1}) + \frac{1}{\epsilon^2}(\frac{1}{2} - \Phi_2^n)(\xi^n + \eta^n)\big), 2\xi^{n-\frac{1}{2}}\Big)\Big| \\
&\quad \leq 2\left\|\Big(-\overline{{}_{CH}\mathrm{D}^{\alpha}_{a,t}\eta^n} + \frac{1}{\epsilon^2}(\frac{1}{2} - \Phi_1^n)(\xi^{n-1} + \eta^{n-1}) + \frac{1}{\epsilon^2}(\frac{1}{2} - \Phi_2^n)(\xi^n + \eta^n)\Big)\right\| \|\xi^{n-\frac{1}{2}}\| \\
&\quad \leq 2\left\|\Big(-\overline{{}_{CH}\mathrm{D}^{\alpha}_{a,t}\eta^n} + \frac{1}{\epsilon^2}(\frac{1}{2} - \Phi_1^n)\eta^{n-1} + \frac{1}{\epsilon^2}(\frac{1}{2} - \Phi_2^n)\eta^n\Big)\right\| \|\xi^{n-\frac{1}{2}}\| \\
&\qquad + 2\left(\|(\frac{1}{2} - \Phi_1^n)\xi^{n-1}\| + \|(\frac{1}{2} - \Phi_2^n)\xi^n\|\right)\|\xi^{n-\frac{1}{2}}\| \\
&\quad \leq Ch^2\|\xi^{n-\frac{1}{2}}\| + C\|\xi^{n-\frac{1}{2}}\|^2 \\
&\quad \leq Ch^2\left(\|\overline{{}_{CH}\mathrm{D}^{\alpha}_{a,t}u}\|_2 + \|u^{n-1}\|_2 + \|u^n\|_2\right)\|\xi^{n-\frac{1}{2}}\| \\
&\qquad + 2\left(\|(\frac{1}{2} - \Phi_1^n)\xi^{n-1}\| + \|(\frac{1}{2} - \Phi_2^n)\xi^n\|\right)\|\xi^{n-\frac{1}{2}}\| \\
&\quad \leq Ch^2\|\xi^{n-\frac{1}{2}}\| + C\|\xi^{n-\frac{1}{2}}\|^2.
\end{aligned} \tag{3.14}$$

In view of (3.5), we have

$$\left|2\sum_{e}\int_{\partial e}\frac{\partial u^{n-\frac{1}{2}}}{\partial \vec{n}}\xi^{n-\frac{1}{2}}\mathrm{d}s\right| \leq Ch^2\|\xi^{n-\frac{1}{2}}\|, \tag{3.15}$$

where $u^{n-\frac{1}{2}} = \frac{u^n+u^{n-1}}{2}$.

Through the three estimates above and again using the Cauchy–Schwarz inequality, we obtain

$$\sum_{k=1}^{n} b_{n-k}^{n}(\|\xi^k\|^2 - \|\xi^{k-1}\|^2) \leq C\|\xi^{n-\frac{1}{2}}\|^2 + \left(Ch^2 + \|R_1^n\| + \|R_2^n\| + \|R_3^n\|\right)\|\xi^{n-\frac{1}{2}}\|. \tag{3.16}$$

By applying Lemma 5, the following holds:

$$\|R_1^n\| + \|R_2^n\| + \|R_3^n\| \leq C(\log t_n - \log a)^{-\sigma}N^{-\min\{2,r\sigma\}}. \tag{3.17}$$

Substituting (3.17) into (3.16) indicates that

$$\sum_{k=1}^{n} b_{n-k}^{n}(\|\xi^k\|^2 - \|\xi^{k-1}\|^2) \leq C\|\xi^{n-\frac{1}{2}}\|^2 + C\left(h^2 + (\log t_n - \log a)^{-\sigma}N^{-\min\{2,r\sigma\}}\right)\|\xi^{n-\frac{1}{2}}\|. \tag{3.18}$$

Using the discrete Gronwall inequality (see Theorem B.1) and (A.4), we obtain

$$\|\xi^n\| \leq C(h^2 + N^{-\min\{2,r\sigma\}}), \quad 1 \leq n \leq N. \tag{3.19}$$

Thus, the first assertion of the theorem follows by applying (3.3) and the triangle inequality.

Taking the test function $v_h = -2\Delta_h\xi^{n-\frac{1}{2}}$ in (3.10) and using (3.12), we have

$$\begin{aligned}
&\sum_{k=1}^{n} b_{n-k}^{n}(\|\nabla\xi^k\|^2 - \|\nabla\xi^{k-1}\|^2) + 2\|\Delta_h\xi^{n-\frac{1}{2}}\|^2 \\
&\quad = \Big(P_h(-\overline{{}_{CH}\mathrm{D}_{a,t}^{\alpha}\eta^n} - R_hR_1^n + R_2^n - R_3^n + \frac{1}{\epsilon^2}(\frac{1}{2} - \Phi_1^n)(\xi^{n-1} + \eta^{n-1}) \\
&\qquad + \frac{1}{\epsilon^2}(\frac{1}{2} - \Phi_2^n)(\xi^n + \eta^n)), -2\Delta_h\xi^{n-\frac{1}{2}}\Big) - 2\sum_{e}\int_{\partial e}\frac{\partial u^{n-\frac{1}{2}}}{\partial \vec{n}}\Delta_h\xi^{n-\frac{1}{2}}\mathrm{d}s.
\end{aligned} \tag{3.20}$$

By employing (3.2) and leveraging the projection property (3.3), we derive

$$\begin{aligned}
&\left|\Big(P_h(-\overline{{}_{CH}\mathrm{D}_{a,t}^{\alpha}\eta^n} + \frac{1}{\epsilon^2}(\frac{1}{2} - \Phi_1^n)(\xi^{n-1} + \eta^{n-1}) + \frac{1}{\epsilon^2}(\frac{1}{2} - \Phi_2^n)(\xi^n + \eta^n)), -2\Delta_h\xi^{n-\frac{1}{2}}\Big)\right| \\
&\quad \leq \|\Delta_h\xi^{n-\frac{1}{2}}\|^2 + \left(\|\overline{{}_{CH}\mathrm{D}_{a,t}^{\alpha}\eta^n}\|^2 + \|\frac{1}{\epsilon^2}(\frac{1}{2} - \Phi_1^n)\eta^{n-1}\|^2 + \|\frac{1}{\epsilon^2}(\frac{1}{2} - \Phi_2^n)\eta^n\|^2\right) \\
&\qquad + \frac{1}{\epsilon^2}\left((\frac{1}{2} - \Phi_1^n)\nabla\xi^{n-1} + (\frac{1}{2} - \Phi_2^n)\nabla\xi^n, 2\nabla\xi^{n-\frac{1}{2}}\right) \\
&\quad \leq Ch^4 + \|\Delta_h\xi^{n-\frac{1}{2}}\|^2 + C\|\nabla\xi^{n-\frac{1}{2}}\|^2,
\end{aligned} \tag{3.21}$$

$$\left|(-R_hR_1^n + R_2^n - R_3^n, -2\Delta_h\xi^{n-\frac{1}{2}})\right| \leq 2\left(\|\nabla R_hR_1^n\| + \|\nabla R_2^n\| + \|\nabla R_3^n\|\right)\|\nabla\xi^{n-\frac{1}{2}}\|, \tag{3.22}$$

and

$$\left|-2\sum_{e}\int_{\partial e}\frac{\partial u^{n-\frac{1}{2}}}{\partial \vec{n}}\Delta_h\xi^{n-\frac{1}{2}}\mathrm{d}s\right| \le Ch^4 + \|\Delta_h\xi^{n-\frac{1}{2}}\|^2. \tag{3.23}$$

Thus, it follows from (3.20)–(3.23) that

$$\begin{aligned}&\sum_{k=1}^{n} b_{n-k}^{n}(\|\nabla\xi^k\|^2 - \|\nabla\xi^{k-1}\|^2)\\ &\quad\le 2\left(\|\nabla R_h R_1^n\| + \|\nabla R_2^n\| + \|\nabla R_3^n\|\right)\|\nabla\xi^{n-\frac{1}{2}}\| + Ch^4 + C\|\nabla\xi^{n-\frac{1}{2}}\|^2.\end{aligned} \tag{3.24}$$

By repeating the discussion process of (3.19), we can conclude that

$$\|\nabla\xi^n\| \le C(h^2 + N^{-\min\{2,r\sigma\}}), \quad 1 \le n \le N. \tag{3.25}$$

This, together with (3.4), leads to the following result:

$$\|\nabla(I_h u^n - U_h^n)\| \le \|\nabla(I_h u^n - R_h u^n)\| + \|\nabla\xi^n\| \le C(h^2 + N^{-\min\{2,r\sigma\}}), \quad 1 \le n \le N.$$

The second assertion in the theorem has been proven completed. □

In order to examine the superconvergence of the fully–discrete scheme (3.7), a new mesh family $\hat{\Gamma}_h = \{\hat{e}\}$ is introduced. Each new element $\hat{e}$ in $\hat{\Gamma}_h$ is formed by combining four adjacent elements from the original mesh Γ_h. Let $a_i\,(i = 1, \cdots, 9)$ be the nine vertices of the four small elements. For any element $\hat{e}$ in $\hat{\Gamma}_h$, an interpolation postprocessing operator $\hat{I}_h$ is defined as stated in [50]:

$$\begin{aligned}&\hat{I}_h v|_{\hat{e}} \in Q_{22}(\hat{e}),\\ &\hat{I}_h v(a_i, t) = v(a_i, t), \quad \forall v \in C(\hat{e}),\\ &\hat{I}_h I_h v = \hat{I}_h v, \quad \forall v \in H^2(\Omega),\\ &\|\hat{I}_h v - v\|_1 \le Ch^2\|v\|_3, \quad \forall v \in H^3(\Omega),\\ &\|\hat{I}_h v_h\|_1 \le C\|v_h\|_1, \quad \forall v_h \in V_h,\end{aligned} \tag{3.26}$$

where $Q_{22}(\hat{e}) = \mathrm{span}\{1, x, y, xy, x^2y, xy^2, x^2, y^2, x^2y^2\}$.

Theorem 3. *Assuming that the conditions of Theorem 2 are satisfied, for* $1 \le n \le N$, *we have*

$$\|u^n - \hat{I}_h U_h^n\|_1 \le C(N^{-\min\{2,r\sigma\}} + h^2).$$

Proof. According to the conclusion of Theorem 2 and using (3.26), we deduce that

$$\begin{aligned}\|u^n - \hat{I}_h U_h^n\|_1 &\le \|\hat{I}_h U_h^n - \hat{I}_h I_h u^n\|_1 + \|\hat{I}_h I_h u^n - u^n\|_1\\ &= \|\hat{I}_h(U_h^n - I_h u^n)\|_1 + \|\hat{I}_h u^n - u^n\|_1\\ &\le C(N^{-\min\{2,r\sigma\}} + h^2).\end{aligned}$$

This completes the proof. □

Remark 1. Although, theoretically, in order to achieve second-order accuracy in time, the scheme (3.7) requires the fractional derivative order α to satisfy the condition $0.43845 \approx (5 - \sqrt{17})/2 < \alpha < 1$ (see Theorems 2 and 3), our numerical experiments have shown that this condition is not absolutely necessary. In fact, for all $0 < \alpha < 1$, as long as $r \ge 2/\sigma$, second-order convergence can be achieved. For details, see Example 2.

4. Numerical examples

In this section, we aim to validate the effectiveness and accuracy of the scheme (3.7) for solving the Allen–Cahn equation with a Caputo–Hadamard time derivative through numerical experiments. Furthermore, we conduct numerical simulations of the Allen–Cahn equation using various time derivatives (including the integer order derivative, the Caputo derivative, and the Caputo–Hadamard derivative) to examine the influence of the time derivative on the solution's behavior.

Example 2. *We study the following Allen–Cahn equation:*

$$\begin{cases} {}_{CH}\mathrm{D}^{\alpha}_{1,t}u(\mathbf{x},t) - \Delta u(\mathbf{x},t) + f\big(u(\mathbf{x},t)\big) = g(\mathbf{x},t), & (\mathbf{x},t) \in \Omega \times (1,2], \\ u(\mathbf{x},t) = 0, & (\mathbf{x},t) \in \partial\Omega \times (1,2], \\ u(\mathbf{x},1) = 0, & \mathbf{x} \in \Omega, \end{cases} \tag{4.1}$$

where $\Omega = (0,1) \times (0,1)$. *The function* $g(\mathbf{x},t)$ *is selected to fulfill the exact solution* $u(\mathbf{x},t) = (\log t)^{\alpha}(1-x)(1-e^{-x})y(1-y)$.

It is easy to observe that for Eq. (4.1), the solution exhibits initial weak singularity in time and anisotropic behavior in space. We take the regularization parameter $\sigma = \alpha$ from (2.7). According to Theorem 2 and Theorem 3, to achieve optimal second-order accuracy in time, the grading mesh parameter r should satisfy $r \geq \frac{2}{\alpha}$. In Table 1, we present the errors and temporal convergence rates for different values of α when $r = \frac{2}{\alpha}$, demonstrating that the proposed scheme achieves second-order convergence. Table 2 shows the numerical results in the spatial direction, which are also consistent with the theoretical analysis.

Table 1. Numerical accuracy in the temporal direction of the scheme (3.7) for Example 2, where $r = 2/\alpha$.

		$\alpha = 0.4$		$\alpha = 0.6$		$\alpha = 0.8$	
$\|u^{n+1} - u_h^{n+1}\|$	N	Error	Order	Error	Order	Error	Order
	8	7.8283e-03	–	7.1869e-03	–	6.5747e-03	–
	16	2.0604e-03	1.9258	1.8954e-03	1.9229	1.7396e-03	1.9181
	32	5.2282e-04	1.9785	4.8112e-04	1.9780	4.4187e-04	1.9770
	64	1.3162e-04	1.9900	1.2106e-04	1.9906	1.1115e-04	1.9910
$\|\nabla(I_h u^{n+1} - u_h^{n+1})\|$	N	Error	Order	Error	Order	Error	Order
	8	1.0978e-02	–	9.9169e-03	–	8.8791e-03	–
	16	3.0190e-03	1.8625	2.7222e-03	1.8651	2.4356e-03	1.8661
	32	7.7421e-04	1.9632	6.9737e-04	1.9648	6.2371e-04	1.9653
	64	1.9666e-04	1.9770	1.7683e-04	1.9795	1.5795e-04	1.9814
$\|u^{n+1} - u_h^{n+1}\|_1$	N	Error	Order	Error	Order	Error	Order
	8	1.9520e-02	–	1.7903e-02	–	1.6363e-02	–
	16	4.8534e-03	2.0079	4.4502e-03	2.0083	4.0690e-03	2.0077
	32	1.1988e-03	2.0174	1.0988e-03	2.0180	1.0046e-03	2.0180
	64	2.9982e-04	1.9993	2.7456e-04	2.0007	2.5086e-04	2.0017

Table 2. Numerical accuracy in the spatial direction of the scheme (3.7) for Example 2, where $r = 2/\alpha$.

		$\alpha = 0.4$		$\alpha = 0.6$		$\alpha = 0.8$	
$\|u^{n+1} - u_h^{n+1}\|$	$m \times n$	Error	Order	Error	Order	Error	Order
	8×2	8.0938e-03	–	7.4659e-03	–	6.8638e-03	–
	16×4	2.1444e-03	1.9162	1.9813e-03	1.9139	1.8261e-03	1.9102
	32×8	5.4483e-04	1.9767	5.0355e-04	1.9762	4.6435e-04	1.9754
	64×16	1.3715e-04	1.9901	1.2671e-04	1.9906	1.1681e-04	1.9910
$\|\nabla(I_h u^{n+1} - u_h^{n+1})\|$	$m \times n$	Error	Order	Error	Order	Error	Order
	8×2	1.0594e-02	–	9.6640e-03	–	8.7409e-03	–
	16×4	2.8823e-03	1.8779	2.6271e-03	1.8791	2.3736e-03	1.8807
	32×8	7.3671e-04	1.9680	6.7115e-04	1.9688	6.0617e-04	1.9693
	64×16	1.8701e-04	1.9780	1.7010e-04	1.9802	1.5342e-04	1.9822
$\|u^{n+1} - u_h^{n+1}\|_1$	$m \times n$	Error	Order	Error	Order	Error	Order
	8×2	1.3344e-02	–	1.2175e-02	–	1.1015e-02	–
	16×4	3.1272e-03	2.0931	2.8514e-03	2.0941	2.5779e-03	2.0951
	32×8	7.6641e-04	2.0287	6.9833e-04	2.0297	6.3089e-04	2.0307
	64×16	1.9250e-04	1.9932	1.7511e-04	1.9956	1.5797e-04	1.9978

Example 3. (Mean curvature flow problem [52]) *We study the following equation with Neumann boundary conditions:*

$$\begin{cases} \partial_t^\alpha u(\mathbf{x}, t) - \Delta u(\mathbf{x}, t) + \dfrac{1}{\epsilon^2} f(u(\mathbf{x}, t)) = 0, & (\mathbf{x}, t) \in \Omega \times (a, T], \\ u(\mathbf{x}, a) = \tanh\left(\dfrac{0.25 - \sqrt{(x - 0.5)^2 + (y - 0.5)^2}}{\sqrt{2}\epsilon} \right), & \mathbf{x} \in \Omega, \end{cases} \tag{4.2}$$

where $\Omega = (0, 1) \times (0, 1)$ *and* $\epsilon = 0.01$. *If* $\alpha = 1$, *the operator* $\partial_t^\alpha u(\mathbf{x}, t) = \frac{\partial u(\mathbf{x}, t)}{\partial t}$. *For* $\alpha \in (0, 1)$, $\partial_t^\alpha u(\mathbf{x}, t)$ *can be defined using either the Caputo fractional derivative or the Caputo–Hadamard fractional derivative.*

For the case of $\alpha = 1$, Eq. (4.2) represents the classical Allen–Cahn equation. Figure 3 depicts the changing process of the numerical solution. Clearly, the circle is shrinking as time passes, which is in line with the numerical calculation results in Choi et al. [52].

If the time derivative is the Caputo fractional derivative and $\alpha = 0.4$ and 0.8, the numerical results at $t = 0$, 2, and 10 are shown in Figure 4. As time increases, the circle shrinks. Moreover, the larger the value of α, the faster it shrinks. However, it shrinks more slowly than the integer-order model.

If the time derivative is the Caputo–Hadamard fractional derivative and $\alpha = 0.4$ and 0.8, the numerical results at $t = 1$, 100, and 300 are shown in Figure 5. The circle also shrinks as time goes on. The larger the value of α, the faster it shrinks. But it shrinks more slowly than the Caputo time derivative model.

In conclusion, the shrinking speeds under different derivatives are as follows: integer-order Allen–Cahn equation > Caputo fractional Allen–Cahn equation > Caputo–Hadamard fractional Allen–Cahn equation. In the case of the same fractional derivative, the larger the fractional derivative α, the faster the shrinking. This is consistent with the conclusion obtained by Fan and Li [39].

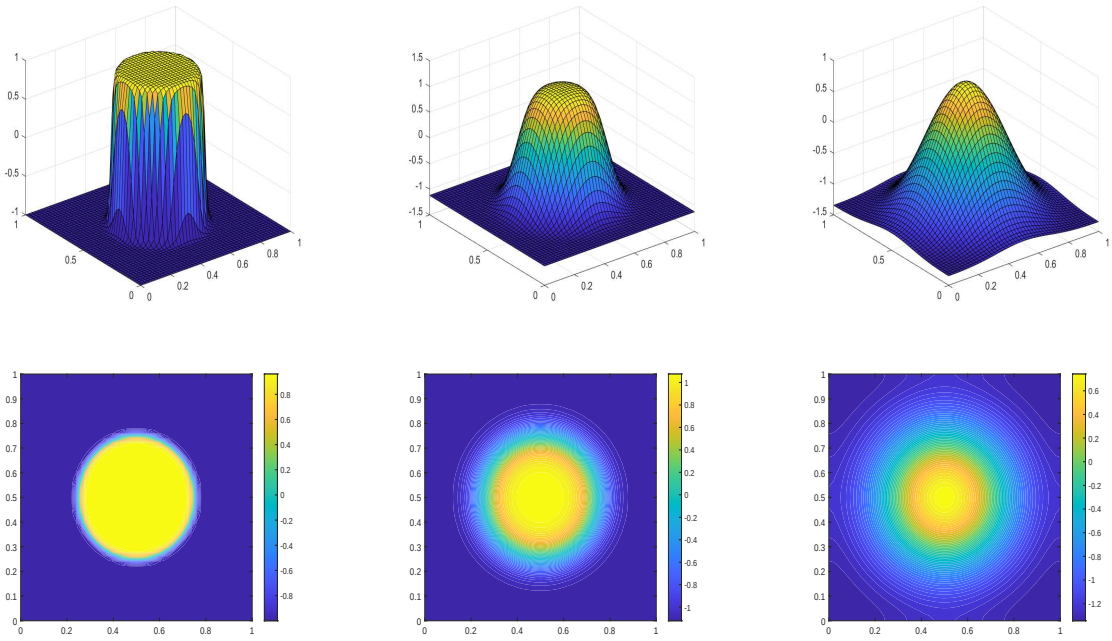

Figure 3. Evolution of numerical solutions for Example 3 with the integer-order time derivative: from left to right corresponding to $t = 0$, 0.2, and 1.

5. Concluding remarks

The primary contributions of this paper are as follows.

(1) We introduce a high-order approximation scheme for approximating the Caputo–Hadamard fractional derivative, known as the nonuniform L1$^+$ formula. When the grading mesh parameter satisfies certain conditions, this method can achieve second-order accuracy.

(2) We explore a numerical algorithm for the Allen–Cahn equation with time as the Caputo–Hadamard fractional derivative. The algorithm employs the nonuniform L1$^+$ formula for temporal discretization and uses the nonconforming quasi-Wilson FEM for spatial approximation. We analyze the error of the algorithm in the L^2-norm and the superclose error in the H^1-norm. Furthermore, by applying interpolation postprocessing techniques, we demonstrate global superconvergence results in the H^1-norm.

(3) Numerical experiments validate the theoretical convergence rates. Furthermore, we numerically solve the Allen–Cahn equation with different types of time derivatives, including integer-order derivatives, Caputo derivatives, and Caputo–Hadamard derivatives, to observe their diffusion processes. The results indicate that the relationship of diffusion speed is as follows: integer-order Allen–Cahn equation > Caputo fractional Allen–Cahn equation > Caputo–Hadamard fractional Allen–Cahn equation.

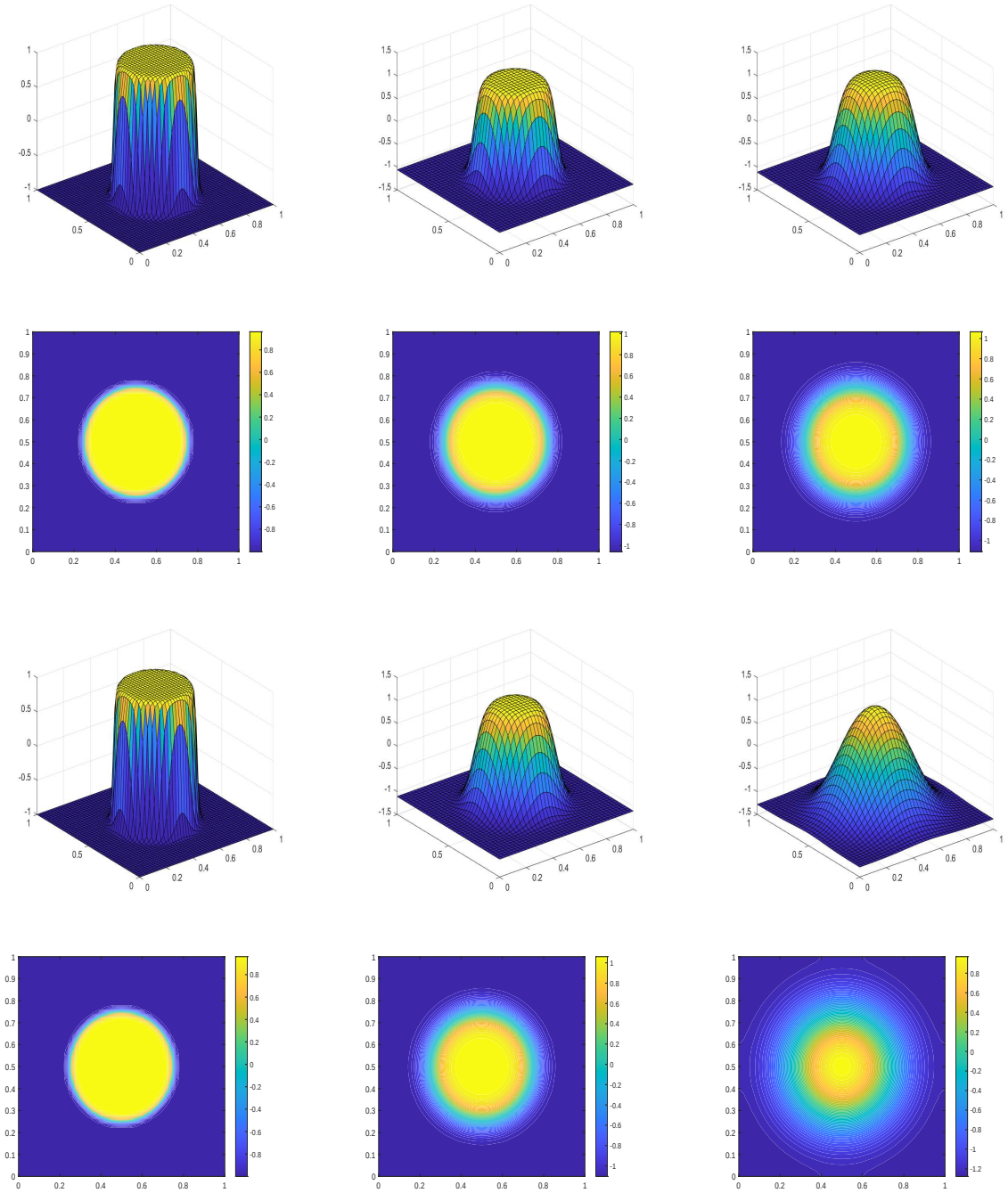

Figure 4. Evolution of numerical solutions for Example 3 with the Caputo time derivative. From left to right, corresponding to $t = 0$, 2, and 10; the top two rows correspond to $\alpha = 0.4$, and the bottom two rows correspond to $\alpha = 0.8$.

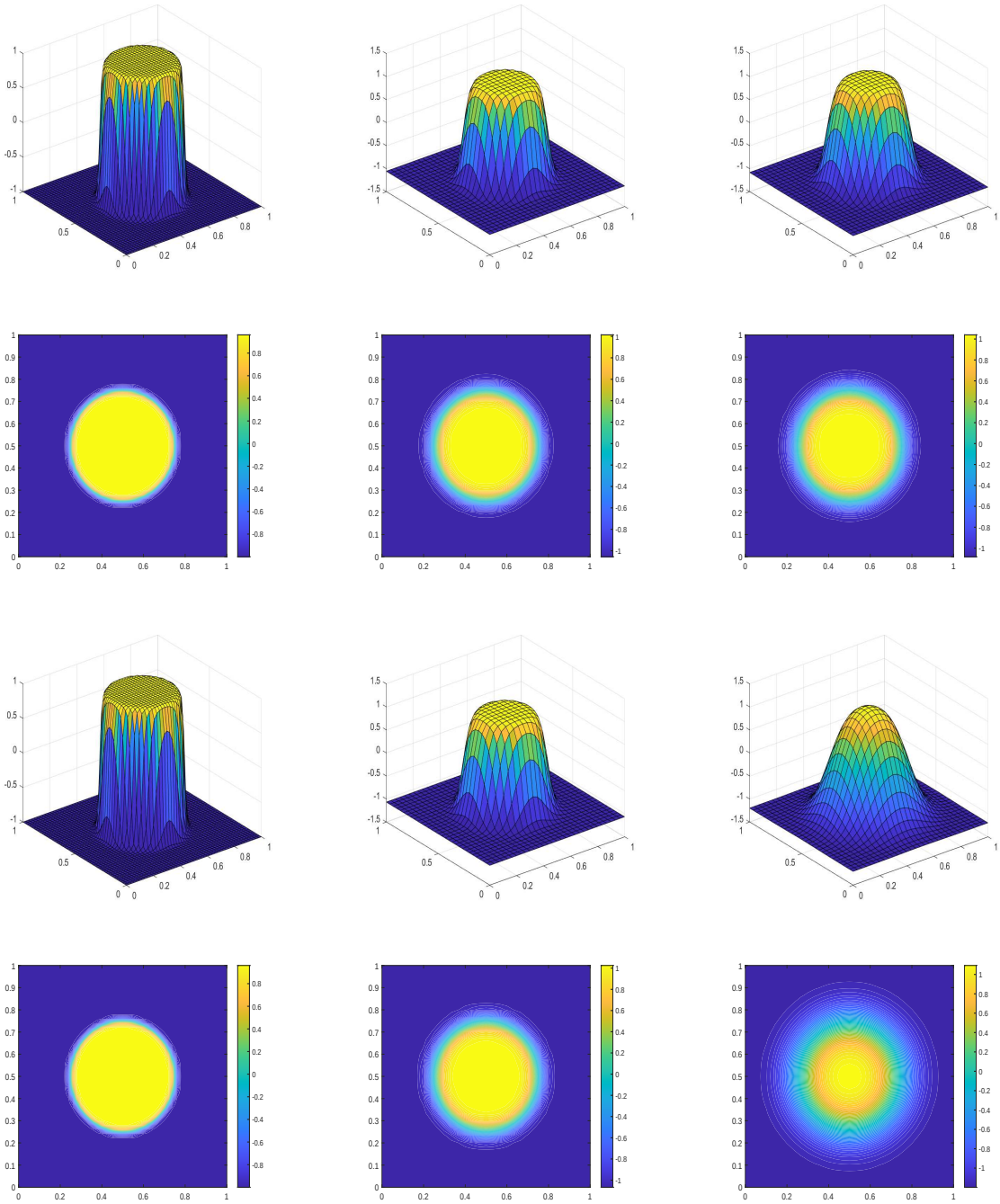

Figure 5. Evolution of numerical solutions for Example 3 with the Caputo–Hadamard time derivative. From left to right, corresponding to $t = 1$, 100, and 300; the top two rows correspond to $\alpha = 0.4$, and the bottom two rows correspond to $\alpha = 0.8$.

Author contributions

Luhan Sun: Writing-original draft; Zhen Wang: Writing-review & editing, Methodology; Yabing Wei: Validation.

Use of AI tools declaration

The authors declare they have not used Artificial Intelligence (AI) tools in the creation of this article.

Acknowledgments

The research of Zhen Wang is supported by the National Natural Science Foundation of China (No. 12101266). The research of Yabing Wei is supported by the Natural Science Foundation of Jiangsu Province (No. BK20240832).

Conflict of interest

The authors declare there is no conflict of interest.

Appendix

A. Properties of the discrete coefficients in (2.5)

Lemma A.1. *For $\alpha \in \left(\frac{5-\sqrt{17}}{2}, 1\right)$, the operator ${}_{CH}\delta^{\alpha}_{a,t}$ defined in (2.6) satisfies*

$$\left({}_{CH}\delta^{\alpha}_{a,t} v^n, v^{n-\frac{1}{2}}\right) \geq \frac{1}{2}\sum_{k=1}^{n} b^n_{n-k}\left(\|v^k\|^2 - \|v^{k-1}\|^2\right).$$

Proof. Following the proof idea of Corollary 1 in [53], the corresponding result can be obtained. □

Lemma A.2. *Define the complementary discrete kernels Q^n_{n-k} $(1 \leq k \leq n)$ as follows:*

$$Q^n_{n-k} = \begin{cases} \frac{1}{b^n_0}, & \text{if } k = n, \\ \frac{1}{b^k_0}\sum_{j=k+1}^{n}(b^j_{j-k-1} - b^j_{j-k})Q^n_{n-j}, & \text{if } k = 1, 2, \cdots, n-1. \end{cases} \tag{A.1}$$

For $\alpha \in \left(\frac{5-\sqrt{17}}{2}, 1\right)$, the following properties hold:
(i)

$$\begin{aligned} &0 \leq Q^n_{n-k} \leq \Gamma(3-\alpha)(\log t_n - \log t_{n-1})^{\alpha}, \quad 1 \leq k \leq n \leq N, \\ &\sum_{k=1}^{n} Q^n_{n-k} \leq (2-\alpha)\Gamma(1-\alpha)(\log t_n - \log a)^{\alpha}, \quad 1 \leq n \leq N, \end{aligned} \tag{A.2}$$

$$\sum_{k=1}^{n} Q^n_{n-k}\omega_{1-\alpha}(\log t_k - \log s) \leq 2-\alpha, \quad 1 \leq n \leq N, \tag{A.3}$$

and

$$\begin{aligned}
&\sum_{k=1}^{n} Q_{n-k}^{n} k^{r(\gamma-\alpha)} \leq \frac{(2-\alpha)\Gamma(1+\gamma-\alpha)}{\Gamma(1+\gamma)}\left(\frac{T-a}{a}\right)^{\alpha} N^{r(\gamma-\alpha)}\left(\frac{a(\log t_n-\log a)}{T-a}\right)^{\gamma}, 0<\gamma\leq\alpha.\\
&\sum_{k=1}^{n} Q_{n-k}^{n} k^{r(\gamma-\alpha)} \leq \frac{(2-\alpha)\Gamma(1+\gamma-\alpha)}{\Gamma(1+\gamma)}\left(\frac{T-a}{T}\right)^{\alpha} N^{r(\gamma-\alpha)}\left(\frac{T(\log t_n-\log a)}{T-a}\right)^{\gamma}, \alpha<\gamma<1.
\end{aligned} \tag{A.4}$$

(ii) Consider a function $v:[a,T]\to\mathbb{R}$ that is continuous and piecewise C^1. If δu is monotonically decreasing and non-negative, then the following holds:

$$\sum_{k=1}^{n-1} Q_{n-k}^{n}\overline{{}_{CH}\mathrm{D}_{a,t}^{\alpha} v(t_k)} \leq (2-\alpha)\int_a^{t_n}\delta v(s)\frac{\mathrm{d}s}{s}, \quad 1\leq n\leq N. \tag{A.5}$$

(iii) For any real number $\mu>0$, we have

$$\sum_{k=1}^{n-1} Q_{n-k}^{n} E_{\alpha}\left(\mu(\log t_k-\log a)^{\alpha}\right) \leq \frac{(2-\alpha)\left(E_{\alpha}\left(\mu(\log t_n-\log a)^{\alpha}\right)-1\right)}{\mu}, \quad 1\leq n\leq N-1.$$

Here, $E_{\alpha}=\sum_{k=0}^{\infty}\frac{z^k}{\Gamma(k\alpha+1)}$ represents the Mittag–Leffler function.

Proof. (i) Applying Lemma 1 (ii), (A.2) is proven. Since $Q_{n-k}^{n} b_0^k \leq \sum_{j=k}^{n} Q_{n-j}^{n} b_{j-k}^{j}=1$, then $Q_{n-k}^{n}\leq \frac{1}{b_0^k}\leq \Gamma(3-\alpha)(\log t_n-\log a)^{\alpha}$. Because $\omega_{1-\alpha}(\log t_j-\log a)$ is monotonically decreasing, we have $\sum_{k=1}^{n} Q_{n-k}^{n}\omega_{1-\alpha}(\log t_n-\log a)\leq\sum_{k=1}^{n} Q_{n-k}^{n}\omega_{1-\alpha}(\log t_k-\log a)\leq(2-\alpha)\sum_{k=1}^{n} Q_{n-k}^{n} b_{k-1}^{k}=2-\alpha$, yielding (A.3). Similar to the proof of Lemma 3.5 in [18], it can be seen that (A.4) holds.

(ii) Using Lemma 1 (ii) and Lemma A.2, we obtain

$$\begin{aligned}
&\overline{{}_{CH}\mathrm{D}_{a,t}^{\alpha} v(t_k)}\\
&=\frac{1}{\log t_k-\log t_{k-1}}\int_{t_{k-1}}^{t_k}{}_{CH}\mathrm{D}_{a,t}^{\alpha} v(t_k)\frac{\mathrm{d}t}{t}\\
&=\frac{1}{\log t_k-\log t_{k-1}}\int_{a}^{t_k}\int_{t_{k-1}}^{t_k}\omega_{1-\alpha}(\log t_k-\log s)\frac{\mathrm{d}t}{t}\delta v(s)\frac{\mathrm{d}s}{s}\\
&\leq\frac{1}{\log t_k-\log t_{k-1}}\sum_{j=1}^{k}\int_{t_{j-1}}^{t_j}\int_{t_{k-1}}^{t_k}\omega_{1-\alpha}(\log t_k-\log s)\frac{\mathrm{d}t}{t}\frac{\mathrm{d}s}{s}\int_{t_{j-1}}^{t_j}\delta v(s)\frac{\mathrm{d}s}{s}\frac{1}{\log t_j-\log t_{j-1}}\\
&\leq(2-\alpha)\sum_{j=1}^{k} b_{k-j}^{k}\int_{t_{j-1}}^{t_j}\delta v(s)\frac{\mathrm{d}s}{s}.
\end{aligned}$$

Thus,

$$\begin{aligned}
\sum_{k=1}^{n} Q_{n-k}^{n}\overline{{}_{CH}\mathrm{D}_{a,t}^{\alpha} v(t_k)} &\leq (2-\alpha)\sum_{k=1}^{n} Q_{n-k}^{n}\sum_{j=1}^{k} b_{k-j}^{k}\int_{t_{j-1}}^{t_j}\delta v(s)\frac{\mathrm{d}s}{s}\\
&=(2-\alpha)\sum_{j=1}^{n}\int_{t_{j-1}}^{t_j}\delta v(s)\frac{\mathrm{d}s}{s}\sum_{k=j}^{n} Q_{n-k}^{n} b_{k-j}^{k}\leq(2-\alpha)\int_a^{t_n}\delta v(s)\frac{\mathrm{d}s}{s}.
\end{aligned}$$

(iii) The proof process closely mirrors that of Lemma 3.4 in [23], which is omitted here for brevity. □

B. Gronwall inequality

Theorem B.1. *Let* $\{\lambda_k\}_{k=0}^{N-1}$ *be a non-negative sequence, and a constant* Λ *exists such that* $\sum_{k=0}^{N-1}\lambda_k \le \Lambda$. *Let* $\{\xi^n, \eta^n : 1 \le n \le N\}$ *be non-negative sequences, and the grid function* $\{v^n : n \ge 0\}$ *satisfies the condition*

$$\sum_{k=1}^{n} b_{n-k}^{n}\left((v^k)^2 - (v^{k-1})^2\right) \le \sum_{s=1}^{n} \lambda_{n-s}(v^{s-\frac{1}{2}})^2 + \xi^n v^{n-\frac{1}{2}} + (\eta^n)^2, \quad 1 \le n \le N.$$

If $\log t_N - \log t_{N-1} \le (2(2-\alpha)\Gamma(3-\alpha)\Lambda)^{-1/\alpha}$, *then the following conclusion holds*

$$v^n \le 2E_\alpha(2\Lambda(\log t_n - \log a)^\alpha)\left(v^0 + \max_{1\le j\le n}\sum_{i=1}^{j} Q_{j-i}^{j}(\xi^i + \eta^i) + \max_{1\le i\le n}\{\eta^i\}\right).$$

Proof. The proof of the lemma follows a similar approach to that outlined in Lemma 3.6 of [18] and is thus omitted here. □

References

1. I. Podlubny, *Fractional Differential Equations*, Academic Press, San Diego, 1999.
2. A. A. Kilbas, H. M. Srivastava, J. J. Trujillo, *Theory and Applications of Fractional Differential Equations*, Elsevier, Amsterdam, 2006.
3. C. P. Li, M. Cai, *Theory and Numerical Approximations of Fractional Integrals and Derivatives*, SIAM, Philadelphia, 2019.
4. R. Garra, F. Mainardi, G. Spada, A generalization of the Lomnitz logarithmic creep law via Hadamard fractional calculus, *Chaos, Solitons Fractals*, **102** (2017), 333–338. https://doi.org/10.1016/j.chaos.2017.03.032
5. E. Y. Fan, C. P. Li, Z. Q. Li, Numerical approaches to Caputo-Hadamard fractional derivatives with applications to long-term integration of fractional differential systems, *Commun. Nonlinear Sci. Numer. Simul.*, **106** (2022), 106096. https://doi.org/10.1016/j.cnsns.2021.106096
6. M. Cai, G. E. Karniadakis, C. P. Li, Fractional SEIR model and data-driven predictions of COVID-19 dynamics of Omicron variant, *Chaos*, **32** (2022), 071101. https://doi.org/10.1063/5.0099450
7. B. Ahmad, A. Alsaedi, S. K. Ntouyas, J. Tariboon, *Hadamard-Type Fractional Differential Equations, Inclusions and Inequalities*, Springer, Switzerland, 2017.
8. D. D. Cao, C. P. Li, Analysis and computation for quenching solution to the time-space fractional Kawarada problem, *Fract. Calc. Appl. Anal.*, **28** (2025), 559–606. https://doi.org/10.1007/s13540-025-00384-7
9. D. D. Cao, C. P. Li, Quenching phenomenon in the Caputo-Hadamard time-fractional Kawarada problem: Analysis and computation, *Math. Comput. Simulat.*, **233** (2025), 21–38. https://doi.org/10.1016/j.matcom.2025.01.014
10. R. Zhu, Z. Wang, Z. Zhang, Global existence and convergence of the solution to the nonlinear ψ-Caputo fractional diffusion equation, *J. Nonlinear Sci.*, **35** (2025), 36. https://doi.org/10.1007/s00332-025-10129-8

11. Z. Wang, L. Sun, The Allen-Cahn equation with a time Caputo-Hadamard derivative: Mathematical and Numerical Analysis, *Communications in Analysis and Mechanics*, **15** (2023), 611–637. https://doi.org/10.3934/cam.2023031
12. M. Gohar, C. P. Li, Z. Q. Li, Finite difference methods for Caputo-Hadamard fractional differential equations, *Mediterr. J. Math.*, **17** (2020), 194. https://doi.org/10.1007/s00009-020-01605-4
13. C. P. Li, Z. Wang, The local discontinuous Galerkin finite element methods for Caputo-type partial differential equations: Mathematical analysis, *Appl. Numer. Math.*, **150** (2020), 587–606. https://doi.org/10.1016/j.apnum.2019.11.007
14. T. G. Zhao, C. P. Li, D. X. Li, Efficient spectral collocation method for fractional differential equation with Caputo-Hadamard derivative, *Fract. Calc. Appl. Anal.*, **26** (2023), 2903–2927. https://doi.org/10.1007/s13540-023-00216-6
15. C. X. Ou, D. K. Cen, S. Vong, Z. B. Wang, Mathematical analysis and numerical methods for Caputo-Hadamard fractional diffusion-wave equations, *Appl. Numer. Math.*, **177** (2022), 34–57. https://doi.org/10.1016/j.apnum.2022.02.017
16. C. X. Ou, D. K. Cen, Z. B. Wang, S. Vong, Fitted schemes for Caputo-Hadamard fractional differential equations, *Numer. Algorithms*, **97** (2024), 135–164. https://doi.org/10.1007/s11075-023-01696-6
17. Z. Wang, L1/LDG method for Caputo-Hadamard time fractional diffusion equation, *Commun. Appl. Math. Comput.*, **7** (2025), 203–227. https://doi.org/10.1007/s42967-023-00257-x
18. Z. Wang, A nonuniform L2-1_σ/LDG method for the Caputo-Hadamard time-fractional convection-diffusion equation, *Adv. Studies: Euro-Tbilisi Math. J.*, **16** (2023), 89–115. https://doi.org/10.32513/asetmj/193220082328
19. C. P. Li, Z. Q. Li, Stability and logarithmic decay of the solution to Hadamard-type fractional differential equation, *J. Nonlinear Sci.*, **31** (2021), 31. https://doi.org/10.1007/s00332-021-09691-8
20. X. C. Zheng, Logarithmic transformation between (variable-order) Caputo and Caputo-Hadamard fractional problems and applications, *Appl. Math. Lett.*, **121** (2021), 107366. https://doi.org/10.1016/j.aml.2021.107366
21. A. Alikhanov, C. Huang, A class of time-fractional diffusion equations with generalized fractional derivatives, *J. Comput. Appl. Math.*, **414** (2022), 114424. https://doi.org/10.1016/j.cam.2022.114424
22. Z. Wang, L. H. Sun, A numerical approximation for the Caputo-Hadamard derivative and its application in time-fractional variable-coefficient diffusion equation, *Discrete Contin. Dyn. Syst., Series S*, **17** (2024), 2679–2705. https://doi.org/10.3934/dcdss.2024027
23. Z. Wang, L. H. Sun, Y. B. Wei, Superconvergence analysis of the nonconforming FEM for the Allen-Cahn equation with time Caputo-Hadamard derivative, *Phys. D*, **465** (2024), 134201. https://doi.org/10.1016/j.physd.2024.134201
24. K. Mustapha, An L1 approximation for a fractional reaction-diffusion equation, a second-order error analysis over time-graded meshes, *SIAM J. Numer. Anal.*, **58** (2020), 1319–1338. https://doi.org/10.1137/19M1260475

25. B. Ji, H. L. Liao, Y. Z. Gong, L. M. Zhang, Adaptive second-order Crank-Nicolson time-step schemes for time-fractional molecular beam epitaxial growth models, *SIAM J. Sci. Comput.*, **42** (2020), B738–B760. https://doi.org/10.1137/19M1259675

26. H. L. Liao, N. Liu, P. Lyu, Discrete gradient structure of a second-order variable-step method for nonlinear integro-differential models, *SIAM J. Numer. Anal.*, **61** (2023), 2157-2181. https://doi.org/10.1137/22M1520050

27. Y. Yan, B. A. Egwu, Z. Liang, Y. Yan, Error estimates of a continuous Galerkin time step method for subdiffusion problem, *J. Sci. Comput.*, **88** (2021), 1–30. https://doi.org/10.1007/s10915-021-01587-9

28. F. Yu, M. H. Chen, Second-order error analysis for fractal mobile/immobile Allen-Cahn equation on graded meshes, *J. Sci. Comput.*, **96** (2023), 49. https://doi.org/10.1007/s10915-023-02276-5

29. J. Y. Shen, F. H. Zeng, M. Stynes, Second-order error analysis of the averaged L1 scheme for time-fractional initial-value and subdiffusion problems, *Sci. China Math.*, **67** (2024), 1641–1664. https://doi.org/10.1007/s11425-022-2078-4

30. S. M. Allen, J. W. Cahn, A microscopic theory for antiphase boundary motion and its application to antiphase domain coarsening, *Acta Metall.*, **27** (1979), 1085–1095. https://doi.org/10.1016/0001-6160(79)90196-2

31. L. Golubović, A. Levandovsky, D. Moldovan, Interface dynamics and far-from-equilibrium phase transitions in multilayer epitaxial growth and erosion on crystal surfaces: Continuum theory insights, *East Asian J. Appl. Math.*, **1** (2011), 297–371. https://doi.org/10.4208/eajam.040411.030611a

32. D. Fan, L. Q. Chen, Computer simulation of grain growth using a continuum field model, *Acta Mater.*, **45** (1997), 611–622. https://doi.org/10.1016/S1359-6454(96)00200-5

33. H. Liu, A. J. Cheng, H. Wang, J. Zhao, Time-fractional Allen-Cahn and Cahn-Hilliard phase-field models and their numerical investigation, *Comput. Math. Appl.*, **76** (2018), 1876–1892. https://doi.org/10.1016/j.camwa.2018.07.036

34. B. Ji, H. L. Liao, L. Zhang, Simple maximum principle preserving time-stepping methods for time-fractional Allen-Cahn equation, *Adv. Comput. Math.*, **46** (2020), 37. https://doi.org/10.1007/s10444-020-09782-2

35. H. L. Liao, T. Tang, T. Zhou, An energy stable and maximum bound preserving scheme with variable time steps for time fractional Allen-Cahn equation, *SIAM J. Sci. Comput.*, **43** (2021), A3503–A3526. https://doi.org/10.1137/20M1384105

36. H. L. Liao, X. Zhu, J. Wang, The variable-step L1 time-stepping scheme preserving a compatible energy law for the time-fractional Allen-Cahn equation, *Numer. Math. Theory Method Appl.*, **15** (2022), 1128–1146. https://doi.org/10.4208/nmtma.OA-2022-0011s

37. H. L. Liao, X. Zhu, H. Sun, Asymptotically compatible energy and dissipation law of the nonuniform L2-1_σ scheme for time fractional Allen-Cahn model, *J. Sci. Comput.*, **99** (2024), 46. https://doi.org/10.1007/s10915-024-02515-3

38. C. Huang, M. Stynes, A sharp α-robust $L^\infty(H^1)$ error bound for a time-fractional Allen-Cahn problem discretised by the Alikhanov L2-1_σ scheme and a standard FEM, *J. Sci. Comput.*, **91** (2022), 43. https://doi.org/10.1007/s10915-022-01810-1

39. E. Y. Fan, C. P. Li, Diffusion in Allen-Cahn equation: Normal vs anomalous, *Phys. D* , **457** (2024), 133973. https://doi.org/10.1016/j.physd.2023.133973
40. F. Jarad, T. Abdeljawad, D. Baleanu, Caputo-type modification of the Hadamard fractional derivatives, *Adv. Differ. Equ.*, **2012** (2012), 1–8. https://doi.org/10.1186/1687-1847-2012-142
41. Y. Q. Long, Y. Xu, Generalized conforming quadrilateral membrane element with vertex rigid rotational freedom, *Comput. Struct.*, **52** (1994), 749–755. https://doi.org/10.1016/0045-7949(94)90356-5
42. J. S. Jiang, X. L. Cheng, A nonconforming element like Wilson's for second order problems, *Math. Numer. Sinica*, **14** (1992), 274–278. https://doi.org/10.12286/jssx.1992.3.274
43. M. Stynes, E. O'Riordan, J. Gracia, Error analysis of a finite difference method on graded mesh for a time-fractional diffusion equation, *SIAM J. Numer. Anal.*, **55** (2017), 1057–1079. https://doi.org/10.1137/16M1082329
44. H. L. Liao, D. Li, J. Zhang, Sharp error estimate of nonuniform L1 formula for linear reaction-subdiffusion equations, *SIAM J. Numer. Anal.*, **56** (2018), 1112–1133. https://doi.org/10.1137/17M1131829
45. S. C. Chen, D. Y. Shi, Y. C. Zhao, Anisotropic interpolation and quasi-Wilson element for narrow quadrilateral meshes, *IMA J. Numer. Anal.*, **24** (2004), 77–95. https://doi.org/10.1093/imanum/24.1.77
46. D. Y. Shi, Y. M. Zhao, F. L. Wang, Quasi-Wilson nonconforming element approximation for nonlinear dual phase lagging heat conduction equations, *Appl. Math. Comput.*, **243** (2014), 454–464. https://doi.org/10.1016/j.amc.2014.05.083
47. S. C. Chen, D. Y. Shi, Accuracy analysis for quasi-Wilson element, *Acta Math. Sci.*,**20** (2000), 44–48. https://doi.org/10.1016/S0252-9602(17)30730-0
48. V. Thomée, *Galerkin Finite Element Methods for Parabolic Problems, second ed.,* Springer, Berlin, 2006.
49. D. Y. Shi, P. L. Wang, Y. M. Zhao, Superconvergence analysis of anisotropic linear triangular finite element for nonlinear Schrödinger equation, *Appl. Math. Lett.*, **38** (2014), 129–134. https://doi.org/10.1016/j.aml.2014.07.019
50. Q. Lin, J. F. Lin, *Finite Element Methods: Accuracy and Improvement*, Elsevier, 2006.
51. B. Zhou, X. Chen, D. Li, Nonuniform Alikhanov linearized Galerkin finite element methods for nonlinear time-fractional parabolic equations, *J. Sci. Comput.*, **85** (2020), 39. https://doi.org/10.1007/s10915-020-01350-6
52. J. Choi, H. Lee, D. Jeong, J. Kim, An unconditionally gradient stable numerical method for solving the Allen-Cahn equation, *Physica A*, **388** (2009), 1791–1803. https://doi.org/10.1016/j.physa.2009.01.026
53. A. A. Alikhanov, A new difference scheme for the time fractional diffusion equation, *J. Comput. Phys.*, **280** (2015), 424–438. https://doi.org/10.1016/j.jcp.2014.09.031

AIMS Press